

Cul3 regulates cyclin E1 protein abundance via a degron located within the N-terminal region of cyclin E

Brittney Davidge<sup>1,4</sup>, Katia Graziella de Oliveira Rebola<sup>1</sup>, Larry N. Agbor<sup>2,3</sup>, Curt D. Sigmund<sup>2</sup> and Jeffrey D. Singer<sup>1\*</sup>

<sup>1</sup>Department of Biology, Portland State University, Portland, Oregon 97201, USA

<sup>2</sup>Department of Physiology, Medical College of Wisconsin, Milwaukee, Wisconsin, USA

<sup>3</sup>Present address: Danish Myograph Technology (DMT), Ann Arbor, Michigan, USA

<sup>4</sup>Present address: Center for Global Infectious Disease Research, Seattle Children's Research Institute, Seattle, Washington, USA

**\*Corresponding Author: [jsinger@pdx.edu](mailto:jsinger@pdx.edu)**

**Key words:** Cul3; cyclin E; cancer, G1/S transition, ubiquitin

**Summary Statement:** Cyclin E is targeted by Cul3 for proteasomal degradation via a newly-identified degron located within the N-terminal domain of cyclin E, a region that is often missing in cancer cells.

**Abstract:**

Cyclin E and its binding partner Cdk2 control the G1/S transition in mammalian cells. Increased levels of cyclin E are found in some cancers. Additionally, proteolytic removal of the cyclin E N-terminus occurs in some cancers and is associated with increased cyclin E/Cdk2 activity and poor clinical prognosis. Cyclin E levels are tightly regulated and controlled in part through ubiquitin-mediated degradation initiated by one of two E3 ligases, Cul1 and Cul3. Cul1 ubiquitinates phosphorylated cyclin E, but the mechanism Cul3 uses to ubiquitinate cyclin E is poorly understood. To ascertain how Cul3 mediates cyclin E destruction, we identified a degron on cyclin E that Cul3 targets for ubiquitination. Recognition of the degron and binding of Cul3 does not require a BTB domain-containing adaptor protein. Additionally, this degron is lacking in N-terminally truncated cyclin E. Our results describe a mechanism whereby N-terminally truncated cyclin E can avoid the Cul3 degradation pathway. This mechanism helps to explain the increased activity that is associated with the truncated cyclin E variants that occur in some cancers.

**Introduction:**

Cyclin E and its binding partner Cdk2 regulate the transition from G<sub>1</sub> to S-phase and release from quiescence in mammalian cells (Koff et al., 1991, Geng et al., 2003). Thus, it is not surprising that cell cycle errors are associated with alterations to cyclin E function and/or abundance; fibroblasts lacking both cyclin E genes, cyclin E1 and cyclin E2, are unable to release from quiescence (Geng et al., 2003). In contrast, overexpression of cyclin E is associated with cancer and tumorigenesis (Said and Medina, 1995). Analysis of the cyclin E protein has revealed several functional domains including a central cyclin homology domain which interacts with Cdk2, a unique N-terminal region, and a C-terminal PEST sequence (residues 385-401), which is commonly found in proteins that get degraded by the ubiquitin system (Lew et al., 1991, Rogers and Rechsteiner, 1986, Rogers et al., 1986, Richardson et al.,

1993, Honda et al., 2005, Rath and Senapati, 2014). In certain cancers, including breast, ovarian and melanoma, cyclin E (50 kilodaltons) is known to be cleaved by proteases resulting in N-terminally truncated low molecular weight (LMW) forms ranging in size from 33 to 45 kilodaltons (Scuderi et al., 1996, Porter and Keyomarsi, 2000, Porter et al., 2001, Harwell et al., 2000, Wang et al., 2003, Libertini et al., 2005). LMW cyclin E activates Cdk2 and demonstrates increased cyclin E/Cdk2 activity (Porter et al., 2001). These forms of cyclin E are associated with poor clinical prognosis in cancer patients (Porter et al., 2001, Harwell et al., 2000, Duong et al., 2012).

Cyclin E expression is restricted to the G<sub>1</sub>/S transition by two distinct E3 ubiquitin ligase complexes which are responsible for the degradation of cyclin E: Cul1 and Cul3 (Clurman et al., 1996, Singer et al., 1999, Strohmaier et al., 2001, Welcker et al., 2003). Both Cul1 and Cul3 are members of the cullin-RING family of ubiquitin ligases. Cul1/SCF (Skp1, Cul1, Fbxw7) based ligases use Fbxw7 as a substrate adaptor to recognize cyclin E (Strohmaier et al., 2001, Koepp et al., 2001, Hao et al., 2007). Cul1 mediated-degradation requires phosphorylation of cyclin E at T77 and T395 in order for ubiquitination of cyclin E to occur (Loeb et al., 2005, Welcker et al., 2003, Clurman et al., 1996, Minella et al., 2008). Cul1-mediated degradation of cyclin E occurs about four hours following release from a thymidine block (S-phase) (Bhaskaran et al., 2013).

In contrast to the Cul1 pathway, the mechanistic details of Cul3 mediated destruction of cyclin E remain largely uncharacterized. Similar to Cul1 complexes, Cul3 ubiquitin ligase complexes consist of a substrate adaptor (BTB domain-containing protein) which binds near the Cul3 N-terminus to recruit substrates, and a C-terminal region that binds to the RING finger protein Rbx1 (Tyers and Jorgensen, 2000, Jin and Harper, 2002, Duda et al., 2008), which in turn, recruits an E2 ubiquitin conjugating enzyme (Petroski and Deshaies, 2005). Previous studies from our lab have shown that Cul3 degrades cyclin E that is not bound to Cdk2 and

regulation of cyclin E by Cul3 is necessary for the maintenance of quiescence in the liver (Singer et al., 1999, McEvoy et al., 2007).

Despite the advances, many details regarding the mechanism utilized by Cul3 for cyclin E ubiquitination remain uncharacterized, including the location of the degron that Cul3 uses to recognize and ubiquitinate cyclin E. A degron is a sequence or structural motif that is required for a protein to be recognized and degraded in a ubiquitin-dependent manner and can include both the ubiquitinated lysine as well as other features required for ubiquitination, such as a binding site (Laney and Hochstrasser, 1999). Here, the Cul3 degron near the N-terminus of cyclin E is identified, and a unique mechanism for Cul3-mediated cyclin E destruction is proposed.

## **Results:**

### **Cyclin E binds directly to Cul3 independently of BTB domain-containing proteins**

Cul3 has been shown to require a BTB domain-containing protein to bind substrates (Pintard et al., 2003, Pintard et al., 2004, Kwon et al., 2006, Geyer et al., 2003, Cummings et al., 2009, Choi et al., 2016, Chen et al., 2009), but previous work from our lab has shown Cul3 binds cyclin E in a yeast two-hybrid screen, indicating that the proteins may interact directly with each other (Singer et al., 1999). In order to determine the nature of the interaction between Cul3 and cyclin E, and whether the two proteins interact directly with each other, several Cul3 mutants were co-transfected with cyclin E and their binding was measured using immunoprecipitation. The mutants represented disruptions of the major functional regions of Cul3: the BTB domain interaction region (residues 51-67), the Nedd8 modification site (K712R), and the gain of function 403-459 deletion (Wimuttisuk et al., 2014, McCormick et al., 2014, Wimuttisuk and Singer, 2007, Zheng et al., 2002, Boyden et al., 2012). Cyclin E bound to all Cul3 mutants tested, including the Cul3 $\Delta$ 51-67 mutant, which cannot bind BTB

proteins (Figure 1A lane 3). This finding is consistent with cyclin E being able to bind directly to Cul3 without the aid of a BTB protein.

In order to further delineate the interaction between Cul3 and cyclin E, Cul3 and cyclin E binding was examined in the presence of SPOP, a BTB protein that targets other (non-cyclin E) Cul3 substrates for ubiquitination (Kwon et al., 2006, Zhang et al., 2014). First, we compared the ability of cyclin E to bind SPOP in comparison to RhoBTB3 as a control, as RhoBTB3 has been shown to bind cyclin E (Lu and Pfeffer, 2013) (Figure 1B). We determined that cyclin E associates with SPOP only in the presence of Cul3 whereas cyclin E binds RhoBTB3 under all circumstances tested (Figure 1B compare lanes 3 and 5 to lanes 2 and 4). These data suggest that the observed interaction between cyclin E and SPOP can only occur if it is mediated by Cul3 (Figure 1B). To further analyze this relationship, cyclin E and SPOP were co-transfected with WT Cul3 and we observed, as shown in Figure 1C, that cyclin E can co-immunoprecipitate SPOP, however, cyclin E was not able to co-immunoprecipitate SPOP when the Cul3 mutant Cul3 $\Delta$ 51-67, which cannot bind BTB domain-containing proteins, was used (Figure 1C lane 2 compared to lane 3). These data demonstrate that Cul3 can link cyclin E to SPOP as immunoprecipitation of SPOP by cyclin E occurs only when SPOP is bound to Cul3. These data support the hypothesis that a direct interaction occurs between cyclin E and Cul3 and also indicate that the interaction between Cul3 and cyclin E occurs outside of the BTB binding region on Cul3.

### **Mutations in the N-terminal region of cyclin E prevent degradation by the Cul3 complex**

To more precisely map the region of cyclin E that binds to Cul3, two C-terminally truncated cyclin E mutants were analyzed for binding to Cul3 and compared to full-length cyclin E. These consisted of the N-terminal 200 amino acids (STOP 200) of cyclin E and the N-terminal 300 amino acids (STOP 300) of cyclin E (Figure 2A). A STOP 100 truncation of cyclin E was also transfected, but it was found to be unstable and therefore not used for further

experimentation (Figure 2A). Cul3 bound to both cyclin E truncation mutants as well as wild type cyclin E (Figure 2B compare lanes 2 and 4 to lane 6), indicating that Cul3 interacts with the N-terminal half of cyclin E. To further pinpoint the binding site, we examined the potential binding of several cyclin E alanine-scanning mutants to Cul3 (Kelly et al., 1998). Each mutant in this set contains a charged amino acid sequence that has been mutated to alanines (Figure 2C). Amongst the set of mutants, one alanine-scanning mutant DPDEE→AAAAA (amino acids 41-45), which is located near the N-terminus, showed decreased binding to Cul3 (Figure 2D first panel lane 4 in comparison to lanes 2, 6, and 8).

After determining that Cul3 only requires the N-terminal portion of cyclin E for binding, we sought to ascertain if this region contains all the necessary signals for Cul3-mediated degradation to occur. To efficiently identify the precise interaction region, we utilized a novel transfection assay that we developed using cells that are deficient for Cul3. Cul3 is responsible for the differences in cyclin E protein *abundance* between wild-type MEFs (Mouse Embryonic Fibroblasts) and cells deficient for Cul3, as we have previously shown that both cell types express similar levels of cyclin E mRNA (McEvoy et al., 2007). It was observed that in Cul3 hypomorphic (floxed) MEFs, transfected cyclin E was more abundant than in WT MEFs, similar to the endogenous levels of cyclin E (McEvoy et al., 2007). When transfected into the same cells, controls that are not Cul3 substrates express evenly. The same regulation of cyclin E was observed when comparing WT (Cul3 containing) and Cul3 KO HEK293 cells (Ibeawuchi et al., 2015) (Figure 3A lanes 1 and 2). We reasoned that if a mutant cyclin E, that lacked the Cul3 degron, was transfected into these two genotypes, we would not see a difference in levels of cyclin E protein. Therefore, transfected cyclin E mutants that are Cul3 substrates would be expected to express at higher levels in the Cul3 KO cells in comparison to wild-type 293 cells.

Two controls, wild type cyclin E and lysineless cyclin E, were transfected into the two cell types (WT and Cul3 KO 293s). As mentioned above, we observed that when transfected with equal amounts of WT cyclin E, the protein is detected at higher levels in the KO 293 cells than the WT cells (Figure 3A compare lanes 1 and 2). In contrast, lysineless cyclin E was expressed evenly in both cell types (Figure 3A lanes 3 and 4), indicating the utility of this assay as a measure of the substrate being recognized for degradation instead of merely binding. To demonstrate that loss of degradation causes an increase in transfected cyclin E protein abundance, wild-type cyclin E was transfected in the presence and absence of the proteasome inhibitor MG132 (Figure S1). We observed that the level of transfected cyclin E in the WT 293 cells increases in the presence of MG132 (Figure S1).

The relative steady state levels of the cyclin E truncations were examined by transfection into WT and Cul3 KO 293 cells. We observed that both the STOP 200 and STOP 300 cyclin E truncations are more abundant in the KO cells, implying that the degron recognized by Cul3 is within the first half of the cyclin E protein and that the C-terminal PEST sequence (residues 385-401) is not necessary for Cul3-mediated degradation to occur (Figure 3B compare lane 1 to lane 2 and compare lane 3 to lane 4). Taken together, these results demonstrate that the Cul3 degron resides in the N-terminal half of the cyclin.

To further establish the important role of the cyclin E N-terminal domain (residues 1 through 86) in cyclin E ubiquitination by Cul3 a Flag-tagged fusion protein containing residues 2 through 86 of cyclin E was fused to YFP. We observed that the fusion protein is only ubiquitinated when both Cul3 and ubiquitin are present (Figure 3C, compare lane 4 to lanes 1 through 3). Conversely, wild-type YFP is not ubiquitinated in this assay (Figure 3C, lanes 5 through 8), thereby demonstrating the specificity of the interaction between Cul3 and the N-

terminal portion of cyclin E, while clearly indicating that the cyclin E N-terminal region alone contains the signals necessary for Cul3-mediated ubiquitination to occur.

### **Lysine 48 on cyclin E is located in a newly-identified degron and serves as a ubiquitination site for Cul3**

To pinpoint specific residues on cyclin E that may be involved in degradation, cyclin E alanine scanning mutants were transfected into the Cul3 WT and KO 293 cells (Kelly et al., 1998). Three alanine-scanning mutants, DPDEE→AAAAA (residues 41-45), KIDR→AIAA (residues 48-51), and DKED→AAAA (residues 79-82), expressed similar levels of protein in the wild-type cells compared to Cul3 knockout cells, which suggests that they are not as easily degraded by Cul3 as wild-type cyclin E (Figure 3D, DPDEE is shown in lanes 1 and 2, KIDR in lanes 3 and 4, and DKED in lanes 5 and 6. WT cyclin E is shown in Figure 3A lanes 1 and 2 for comparison). All three of these mutants are located near the N-terminus of cyclin E. In order to further characterize the importance of this region for Cul3-mediated degradation to occur, two Myc-tagged constructs containing deletions in this region were created (Figure 3E). The first construct, cyclin E $\Delta$ 31-82, is missing the region encompassing the three alanine scanning mutants that demonstrated increased abundance. The second cyclin E deletion construct, cyclin E $\Delta$ 2-86, was designed to resemble the LMW cyclin E found in some cancer cells and is missing the entire N-terminal region (Figure 3E). These mutants both expressed at similar levels in WT cells and Cul3 knockout cells (Figure 3F, compare lane 1 to 2, and lane 3 to lane 4), suggesting that residues 31 through 82 on cyclin E are necessary for Cul3-mediated degradation of cyclin E to occur.

Changes in abundance exhibited by mutant proteins can often be explained by changes in the location of the protein within the cell. In order to determine if the phenotypes of the three, stable, alanine-scanning mutants are the result of localization changes, HeLa cells were



transfected with each construct and visualized using immunofluorescent microscopy. The cellular localization of the three mutants was found to be predominantly nuclear, similar to wild-type cyclin E, indicating that their increased abundance is not caused by mis-localization (Figure S2).

The DPDEE→AAAAA (residues 41-45) mutant cannot bind Cul3 as well as other cyclin E constructs (Figure 2D), which could provide a partial explanation for its increased protein levels in our assay. The other two mutants, KIDR→AIAA (residues 48-51) and DKED→AAAA (residues 79-82) both contain lysine residues (Figure 3D). The increased protein levels of these alanine scanning mutants as well as cyclin E $\Delta$ 31-82 imply that both lysine residues K48 and K80 are potential ubiquitination sites, and the degron that is recognized by Cul3 likely resides within the region spanned by the cyclin E $\Delta$ 31-82 deletion.

To establish if ubiquitination on K48 or K80 of cyclin E regulates its relative expression levels, we determined if the alanine scanning mutants were stabilized by a dominant negative mutation in ubiquitin that prevents K48 branching, a type of branching that leads to degradation (Raasi and Pickart, 2005). We have shown that this ubiquitin mutation results in stabilization of cyclin E whereas a mutation in another important lysine in ubiquitin, lysine 63, has no effect (Figure S3). To examine this, all of the alanine scanning mutants within the first 200 amino acids of cyclin E were transfected into both cell types in the presence or absence of a mutant K48R ubiquitin. We observed that, unlike WT cyclin E which was stabilized in WT cells by the addition of the dominant-negative K48R ubiquitin mutant (Figure 4A, compare lanes 1 and 2 to lanes 3 and 4), the KIDR (48-51)→AIAA mutant was unaffected indicating it is no longer a substrate for ubiquitination-dependent degradation (Figure 4A, lanes 13-16). The DPDEE (41-45)→AAAAA (Figure 4A, lanes 9-12) mutant behaved similarly to the KIDR (48-51)→AIAA mutant. The DKED (79-82)→AAAA mutant (Figure 4A, lanes 17-20) appears similar to wild-type (Figure 4A, top left panel, lanes 1-4), in this assay suggesting K48 (the

KIDR lysine) and not K80 (the DKED lysine) is the ubiquitination site for Cul3. As a second control, cyclin E T395A, which cannot be degraded by Cul1, was examined and we observed that it is a substrate of Cul3 which demonstrates the specificity of our assay (Figure 4A, lanes 5 through 8). In order to confirm that K48 is a ubiquitination site on cyclin E, a point mutant, cyclin E K48R, was constructed for use in the ubiquitination assay. Like the KIDR (48-51) alanine scanning mutant, cyclin E K48R is more stable in WT cells than WT cyclin E (Figure 4A, lanes 21 through 24), suggesting that K48 on cyclin E is indeed a ubiquitination site utilized by Cul3 *in vivo*. These data suggest the presence of a Cul3 degron on cyclin E located near the cyclin E N-terminus. The residues DPDEE (41-45) and KIDR (48-51) constitute the Cul3 binding site (DPDEE) and the ubiquitination site (KIDR) utilized by Cul3 to target cyclin E for ubiquitin-mediated proteolysis.

Previous work from our lab has shown that Cul3 regulates endogenous cyclin E, as wild-type cyclin E has a longer half-life in cells that are deficient for Cul3 and this longer half-life is not associated with changes in mRNA levels of either cyclin E1 or cyclin E2 (McEvoy et al., 2007). To determine if cyclin E K48R is differentially degraded by Cul3 when compared to wild-type cyclin E, we measured the half-life of these proteins in cells of both genotypes (Cul3 WT and KO). Cells were transfected with full-length Myc-tagged cyclin E or Myc-tagged cyclin E K48R. Following addition of cycloheximide (CHX) the cells were harvested every two hours for eight hours. We observed that WT cyclin E has a short half-life in the WT cell line but a dramatically increased half-life in the KO cells, demonstrating that loss of Cul3 increases the half-life of cyclin E (Figure 4B compare WT cyclin E in WT cells (top, left), and WT cyclin E in KO cells (bottom, left)). Next, we measured the half-life of the cyclin E mutant K48R, the putative ubiquitination site. Cyclin E K48R had a half-life longer than WT cyclin E in both WT and Cul3 KO cells, demonstrating that K48 on cyclin E is required for Cul3-

mediated degradation to occur (Figure 4B and 4C, compare the half-life of WT cyclin E (4B) to cyclin E K48R (4C)).

### **The N-terminal domain of cyclin E is required for Cul3-mediated degradation**

As low molecular weight (LMW) cyclin E can be found endogenously in some cells, we sought to determine if loss of Cul3 affects the presence of these LMW forms. Overall, the Cul3 KO 293 cells have more endogenous cyclin E than the wild-type (Ibeawuchi et al., 2015). We observed that the 50 kDa endogenous cyclin E band increases upon inhibition of the proteasome in WT cells to equal the amount of the 50 kDa protein that is present in the KO cells prior to proteasome inhibition, demonstrating that the 50 kDa band is a substrate of Cul3 in 293 cells (Figure 5A lane 2 vs lane 3). Two LMW cyclin E bands are also detected, the smallest of which is about 43 kDa. These two LMW cyclin E bands are present in both WT and KO cells (Figure 5A). The relative abundance of the LMW bands is elevated equally in both cell types upon proteasome inhibition (Figure 5A lanes 2 and 4), indicating that LMW cyclin E is targeted for ubiquitin-mediated proteolysis equally in both cell types.

Next, to determine if the rate of degradation of LMW cyclin E is impacted by Cul3, Myc-tagged cyclin E $\Delta$ 2-86, which lacks its N-terminal domain, was transfected into WT and Cul3 KO 293 cells. Cycloheximide was added to the samples and time points were collected every two hours over the course of ten hours (Figure 5B). The results of this experiment show that cyclin E $\Delta$ 2-86 has the same half-life in WT and KO cells, demonstrating that Cul3 is unable to regulate the abundance of cyclin E protein that lacks its N-terminal domain (Figure 5B). To further test the role of this degron in Cul3 mediated degradation, we created a YFP fusion protein which contains residues 2 through 86 (the N-terminal region) of cyclin E fused to a Flag-tagged YFP. This cyclin E-YFP fusion protein has a shorter half-life than YFP alone but not in the Cul3 KO cells, consistent with our previous conclusion that the N-terminal domain of cyclin E contains the signals necessary for degradation (Figure S4, A). In addition,

Cul3 can bind the YFP containing protein that contains the Cul3 degron but cannot bind YFP alone (Figure S4, B). These results are consistent with our previous data demonstrating the importance of K48, which is located in the N-terminal region, for Cul3-mediated degradation of cyclin E. Together, these data suggest that Cul3 is unable to regulate the LMW cyclin E truncations that occur *in vivo* and lack the Cul3 degron. LMW cyclin E has been shown to bind Cdk2 and results in increased Cdk2 activity (Porter et al., 2001, Wingate et al., 2005). Our data indicate that LMW cyclin E is not a Cul3 substrate, providing a possible mechanism that LMW cyclin E1 might employ in order to bypass ubiquitination by the Cul3 pathway thereby increasing its availability to bind Cdk2 (Figure 5C).

### **Cyclin E2 lacks the Cul3 degron and is not targeted for degradation by Cul3**

The structure of cyclin E bound to Cdk2 has been determined (Honda et al., 2005), but the published structure only includes amino acids 81-363 of cyclin E, omitting the N-terminal region. Recently, advanced modeling techniques have predicted a structure for the N-terminal region of cyclin E which shows that this portion of the protein is mostly disordered with the notable exception of a predicted alpha helix encompassing the sequence “DEEMAKID” (residues 43-50, Figure 6A) (Rath and Senapati, 2014). Coincidentally, the alanine scanning mutants located within this proposed helix (DPDEE (41-45)→AAAAA and KIDR (48-51)→AIAA) exhibited the most notable phenotypes in our study as DPDEE (41-45) exhibited diminished binding to the Cul3 complex and KIDR (48-51)→AIAA cannot be degraded in a Cul3-dependent manner (Figure 2D, Figure 4 and Figure 6). Our data suggests that this structural motif may form part of the interface on cyclin E, which is responsible for Cul3 interaction and also functions as the Cul3 degron on cyclin E (Figure 6A). The putative helix comprising the Cul3 degron, including the K48 ubiquitination site, is conserved in rodents (Figure 6B), which is notable as Cul3 also regulates cyclin E in mice (Singer et al., 1999, McEvoy et al., 2007).

Mammals contain two cyclin E genes, CCNE1 (cyclin E1) and CCNE2 (cyclin E2), which produce different proteins (Sherr and Roberts, 1999, Geng et al., 2003). The two cyclin E proteins share a high degree of homology and many structural similarities, including the Cdk2 interacting domain (Zariwala et al., 1998). To determine if both cyclin E proteins contain the proposed Cul3 degron we analyzed the net charge of the region by calculating the difference between the number of basic residues and the number of acidic residues and ascertained that the cyclin E1 degron is acidic with a net charge of negative two. The corresponding region on cyclin E2, in contrast, is extremely basic with a net charge of plus four (Figure 6C). A Chou-Fasman algorithm was used to predict possible structures of both cyclin E proteins in the degron region (Chou and Fasman, 1975). This method predicts structural differences in the proposed degron region between the two proteins, revealing what is possibly a helical region in cyclin E1 is potentially an unstructured region in cyclin E2 (Figure 6C, “h” indicates helix and “n” indicates no predicted structure). Taken together, this information suggests that the Cul3 degron comprises a structural feature that is unique to cyclin E1.

Next, to determine if the observed Cul3 mediated degradation of cyclin E is specific to cyclin E1, cyclin E2 was transfected into the WT and KO 293 cells. Cyclin E2 expresses evenly in both cell types, indicating that it does not get degraded by a Cul3-dependent mechanism (Figure 6D, lanes 1 and 3 compared to lanes 2 and 4), and unlike cyclin E1, cyclin E2 does not bind Cul3 in an immunoprecipitation assay (Figure 6E). Lastly, transfected cyclin E2 has a similar half-life in the WT and KO 293 cells, suggesting that it is not a Cul3 substrate (Figure S5). Together these data suggest that Cul3 selectively targets cyclin E1 for Cul3-mediated degradation.

### **Loss of Cul3 results in early accumulation of cyclin E after release from serum starvation**

The Cul1 E3 ligase also targets cyclin E for degradation and does so in a distinct window in the cell cycle, beginning about four hours after the onset of DNA replication (Bhaskaran et al., 2013). In order to ascertain when during the cell cycle loss of Cul3 results in cyclin E accumulation we turned to the Cul3 knockout 293 cells. Previous work from our lab has shown that loss of Cul3 in mouse embryonic fibroblasts (MEFs) results in increased amounts of cyclin E and a greater percentage of cells in S-phase (McEvoy et al., 2007). Similarly, analysis of Cul3 KO 293 cells by flow cytometry showed an increased percentage of cells in S phase when compared to WT 293s (Figure 7A). The observed increase in Cul3 KO cells undergoing DNA replication indicates that the excess cyclin E in the Cul3 KO 293 cells promotes entrance into S-phase. To determine at which time during the cell cycle the Cul3 KO cells begin to accumulate excess cyclin E, both WT and KO cells were synchronized in G<sub>1</sub> via serum starvation and released. The results of this experiment show that KO cells enter S-phase earlier than their wild-type counterparts, as four hours after release into G<sub>1</sub>, only 47.1 percent of synchronized wild-type cells are in S-phase or G<sub>2</sub> but 61.7 percent of Cul3 KO cells have reached this point (Figure 7B, WT cells are shown on the left and KO are shown on the right).

To determine if the early entrance of the KO cells into S-phase is a result of cyclin E accumulation during G<sub>1</sub>, we examined cyclin E accumulation in Cul3 hypomorphic MEFs (mouse embryonic fibroblasts) after serum starvation and release. Cyclin E protein accumulated to significant levels two hours earlier in Cul3 hypomorphic (floxed) MEFs than in WT MEFs (Figure 7C WT, top row, Cul3 hypomorphic flx/flx, middle row). Similarly, cyclin E/Cdk2 kinase activity is also elevated prior to S phase in Cul3 KO 293 cells (Figure 7C, bottom panel). This is consistent with a role for Cul3 in regulation of cyclin E levels in

non-cycling cells, as we had previously observed in an animal model (McEvoy et al., 2007). The early entrance of the Cul3 hypomorphic cells into S-phase suggests Cul3 regulation of cyclin E occurs earlier than the Cul1-mediated regulation of cyclin E that occurs during S-phase (Bhaskaran et al., 2013).

### **Discussion:**

Cyclin E protein accumulates in late G<sub>1</sub>, peaks in early S-phase and rapidly disappears. Increased levels of cyclin E are associated with cell cycle errors and loss of cyclin E in MEFs results in the inability of the cells to exit from quiescence (Said and Medina, 1995, Geng et al., 2003). Research has shown that cyclin E can be proteolytically cleaved resulting in truncated forms of the cyclin, many of which lack portions of the protein near the N-terminus (Wang et al., 2003, Porter et al., 2001). These LMW forms of cyclin E are associated with poor prognosis in cancer patients and overexpression of the LMW cyclin E has also been shown to cause cell cycle errors including chromosome mis-segregation (Akli et al., 2010, Duong et al., 2012, Bagheri-Yarmand et al., 2010). Others have shown that these errors result from the increased ability of LMW cyclin E to bind and activate Cdk2, which increases Cdk2 kinase activity (Porter et al., 2001, Wingate et al., 2005). Healthy cells rely upon degradation of cyclin E protein by the ubiquitin-proteasome system in order to restrict levels of cyclin E. The Cul3 E3 ligase targets cyclin E for degradation, and our work sheds light upon the mechanism utilized by Cul3 to ubiquitinate cyclin E.

We have identified a Cul3 degron in cyclin E1 that spans the acidic region between residues 41 and 51 (DPDEEMAKIDR), located near the N-terminus of the cyclin. This degron consists of a region involved in Cul3 binding (residues 41-45) and a ubiquitinated lysine, K48. The N-terminal region containing the degron has not been shown to be part of the core cyclin E protein and is not necessary for Cdk2 activation to occur (Porter and Keyomarsi, 2000, Porter et al., 2001). Our analysis, as well as those from other investigators, suggest that this acidic

region forms a structural motif within the disordered N-terminal domain on cyclin E1 (Figure 6A) (Rath and Senapati, 2014). In addition, we show that Cul3 uses this structural feature, which is conserved in mammals (Figure 6B), to recognize cyclin E1 for ubiquitination (Figure 6). We demonstrate that the Cul3 degron is specific to cyclin E1, as the corresponding region in cyclin E2 carries a positive (basic) charge (Figure 6C) and levels of cyclin E2 are not affected by deletion of Cul3 (Figures 6D and S5).

Also, and surprisingly, mutation of the Cul3 degron on cyclin E results in a stable cyclin E implying, that in the 293 cells, the Cul3 pathway is the predominant pathway involved in the degradation of cyclin E (Figure 4A, lower right panel and Figure 4C). Mutation of K48 in cyclin E to arginine (K48R) results in stable cyclin E that has a longer half-life than WT cyclin E, implying that K48 is the principal ubiquitination site on cyclin E utilized by Cul3 (Figure 4A lower right panel and Figure 4C). The longer half-life of cyclin E K48R in comparison to WT cyclin E has been seen in multiple experiments (N=4), demonstrating the significance of this result. Similarly, deletion of the cyclin E N-terminus (cyclin E $\Delta$ 2-86) prevents Cul3-mediated degradation of cyclin E (Figure 5B). The half-life of cyclin E1 that cannot be ubiquitinated by Cul3 is longer than the half-life of WT cyclin E, indicating the necessity for Cul3 in cyclin E regulation (Figure 4B compared to Figures 4C and Figure 5B).

LMW cyclin E, which results from proteolytic processing and often lacks portions of the N-terminal region, represents a particularly active form of cyclin E that is made in cancer cells and associated with tumorigenesis (Porter and Keyomarsi, 2000, Keyomarsi et al., 1995, Bagheri-Yarmand et al., 2010, Akli et al., 2004, Akli et al., 2010, Porter et al., 2001). Our data suggest that the loss of the newly identified Cul3 degron may contribute to the increased Cdk2 activity that is observed in cells containing LMW cyclin E (Figure 5C). We constructed a cyclin E deletion mutant, cyclin E $\Delta$ 2-86, that is missing the N-terminal region, similar to the naturally occurring LMW cyclin E variants that lack the majority of the N-terminal domain



(Figure 3E). Like cyclin E K48R, cyclin E $\Delta$ 2-86 is also more stable, suggesting that cyclin E1 that lacks the degron cannot be targeted for degradation by Cul3 (Figure 3F, Figure 5B). This finding suggests that removal of the N-terminal cyclin E degron allows for the bypassing of Cul3-mediated degradation of LMW cyclin E1, resulting in more cyclin E that is available to interact with Cdk2 (Figure 5C). Although LMW cyclin E1 is still a substrate of the ubiquitin system (Delk et al., 2009), our results suggest that it is unable to be degraded in a Cul3-dependent manner (Figure 5A). Levels of endogenous LMW cyclin E are increased upon addition of MG132 in Cul3 KO 293 cells (Figure 5A), which further supports the idea that cyclin E lacking its N-terminal region is not a Cul3 substrate (Figures 5A, 5B and 5C).

In addition to clarifying the mechanistic details regarding Cul3-mediated degradation of cyclin E1, the work presented here also identifies the temporal window during which such degradation occurs. Previous work has shown that loss of Cul3 results in cyclin E accumulation and exit from quiescence in mice (McEvoy et al., 2007), leading us to hypothesize that loss of Cul3 results in earlier increases in cyclin E and entry into S-phase. Here, this hypothesis is supported as cells that are hypomorphic for Cul3 both enter the cell cycle earlier than their WT counterparts and show increased levels of cyclin E and associated kinase activity earlier than wild-type cells following release from serum starvation (Figure 7B and 7C). These data suggest that Cul3 is responsible for maintaining levels of cyclin E early in the cell cycle preceding the start of S-phase, which is in contrast to the Cul1 degradation pathway that degrades cyclin E later during S-phase (Bhaskaran et al., 2013). Taken together, our data suggests that during G1, Cul3 functions to suppress levels of cyclin E via ubiquitination of its N-terminal domain (Figure 5B). Lack of cyclin E regulation by Cul3 during G1 might contribute to the increased cyclin E/Cdk2 activity that has been observed in cancer cells containing LMW cyclin E (Figures 5C and 7D).

Lastly, this study suggests that the mode of recognition of cyclin E1 by Cul3 is unique, as it does not require a substrate adaptor. We show that Cul3 binds cyclin E independently and outside of the BTB binding region (residues 51-67) on Cul3 (Figure 1A and 1C), suggesting that Cul3 does not require a BTB protein in order to ubiquitinate cyclin E1. As other Cul3 substrates are known to require BTB proteins to enhance binding to the Cul3 E3 ligase complex (Zhang et al., 2004, Cummings et al., 2009), our finding that cyclin E can bind Cul3 directly suggests that cyclin E is a unique substrate of Cul3. A search of the literature revealed another Cul3 substrate, HSF2 (Heat Shock Factor 2), that is targeted for degradation upon binding directly to Cul3 via two PEST sequences (Xing et al., 2010). PEST sequences are defined as acidic regions rich in the amino acids D, E, P, S, and T that are flanked by basic residues (Rogers et al., 1986). Our results show that the C-terminal PEST sequence in cyclin E is not required for Cul3-mediated degradation to occur (Figure 3B), however the degron that we identified near the cyclin E N-terminus lies within a region that also satisfies the definition of a PEST sequence (residues 31-51, RKANVTVFLQDPDEEMAKIDR). This observation suggests that a PEST motif facilitates Cul3's ability to recognize cyclin E, demonstrating similarity to the PEST motifs in HSF2 which facilitate its ubiquitination by Cul3 (Xing et al., 2010). Together this information suggests a new mode of cullin substrate recognition whereby Cul3 binds some substrates without the aid of a BTB-domain containing protein. This idea will merit further study to determine what, if any, role BTB proteins might play in instances where Cul3 is responsible for substrate recognition. Others have suggested that the BTB protein RhoBTB3 is involved in cyclin E degradation and knockdown of RhoBTB3 resulted in elevated levels of cyclin E and increased proliferation (Lu and Pfeffer, 2013), which suggests to us that RhoBTB3 might play a non-canonical role in cyclin E ubiquitination.

## **Methods:**

### **Cell culture and transfections**

Cells (HEK 293, HeLa, and MEFs) were maintained in DMEM supplemented with ten percent fetal bovine serum and penicillin/streptomycin. HEK 293 and HeLa cells were split 1:20 for transfection in 6 cm dishes the night before transfection. Transfections were performed using the calcium phosphate precipitation method. For immunoprecipitations and expression level assays, cells were harvested 48 hours post transfection. For HeLa and 293 cells, between 1 and 10  $\mu$ g of plasmid DNA was transfected into each plate. For experiments utilizing MG132 (Sigma, [www.sigmaaldrich.com/catalog/product/mm/474790](http://www.sigmaaldrich.com/catalog/product/mm/474790)), drug was added approximately 18 hours before harvest at a final concentration of 20 $\mu$ M. All transfections were harvested using RIPA buffer supplemented with protease inhibitors and then sonicated before being used for immunoprecipitations or western blots.

### **Plasmids**

All Cul3 mutants (Cul3 K712R, Cul3 $\Delta$ 51-67, and Cul3 $\Delta$ 403-459) were expressed using the same p3x-Flag vector (Sigma) as was wild-type Cul3. Cyclin E mutants were expressed using the CS2+ Myc-tagged expression vector, and a CS2+ S-tagged vector was used for the expression of SPOP. The pCMV3-tag-6 vector (Agilent) was used for construction of the cyclin E-YFP fusion protein shown in figures 3C and S4.

### **Western blotting and immunoprecipitations**

Western blots and immunoprecipitations were conducted as previously described (Wimuttisuk et al., 2014). In short, a sonicated transfection lysate was added to the desired antibody in an Eppendorf tube and brought to a final volume of 500 $\mu$ L. 40 $\mu$ L of IPA sepharose beads were then added to the mixture, and the IPs were placed on a rotator for two hours at room temperature before being rinsed with RIPA buffer, heated in SDS-loading buffer, and run on

an SDS-PAGE gel. The following antibodies were used for immunoprecipitations and/or western blotting: Monoclonal anti-FLAG (Sigma, [www.sigmaaldrich.com/catalog/product/sigma/f1804](http://www.sigmaaldrich.com/catalog/product/sigma/f1804) ), monoclonal anti-Myc (9E10, Santa Cruz), polyclonal anti-c-Myc (A14) (Santa Cruz), S-peptide monoclonal antibody (Fisher, [www.thermofisher.com/antibody/product/S-peptide-Epitope-Tag-Antibody-clone-6-2-Monoclonal/MA1-981](http://www.thermofisher.com/antibody/product/S-peptide-Epitope-Tag-Antibody-clone-6-2-Monoclonal/MA1-981)), monoclonal anti-HA.11 (16B12) (ThermoFisher), polyclonal anti-HA (ThermoFisher, [www.thermofisher.com/antibody/product/HA-Tag-Antibody-Polyclonal/PA1-985](http://www.thermofisher.com/antibody/product/HA-Tag-Antibody-Polyclonal/PA1-985)), polyclonal anti- $\beta$  actin (ThermoFisher, [www.thermofisher.com/antibody/product/beta-Actin-Antibody-Polyclonal/PA1-183](http://www.thermofisher.com/antibody/product/beta-Actin-Antibody-Polyclonal/PA1-183)), polyclonal anti-cyclin E (Singer et al., 1999), polyclonal anti-Cul3 (Singer et al., 1999, McEvoy et al., 2007), and monoclonal anti-cyclin E (HE12, Santa Cruz biotechnology).

### **Half-life determination**

For experiments using cycloheximide (Sigma, [www.sigmaaldrich.com/catalog/product/sigma/c4859](http://www.sigmaaldrich.com/catalog/product/sigma/c4859)), cells were transfected as described and drug was added 24 hours post-transfection at a final concentration of 50  $\mu$ g per milliliter. Cells were then harvested at the time points indicated. Quantification of the western blots for all cycloheximide experiments was done using the FluorChem SP software (Alpha Innotech) or ImageJ (National Institute of Health) and graphs were generated using Microsoft Excel.

### **Immunofluorescence**

Hela cells were grown on coverslips, transfected, followed by incubation in four percent paraformaldehyde/PBS at room temperature for 10 minutes. Cells were then permeabilized using a solution of one percent Triton X-100 with 2mM EGTA and 5mM PIPES, followed by incubation in methanol at -20 degrees for 10 minutes. Cells were then rinsed with PBS and stained overnight with a polyclonal Myc antibody (A14, Santa Cruz). The next day, cells were rinsed and stained with an AlexaFluor 488 conjugated secondary antibody (Abcam,

<http://www.abcam.com/goat-rabbit-igg-hl-alex-a-fluor-488-ab150077.html>) followed by DAPI, rinsed in methanol, and mounted on coverslips for viewing. Microscopy was conducted using a Zeiss M2 microscope and AxioVision software.

### **Flow cytometry**

Proliferating cells were harvested when they were 70 percent confluent. Cells were resuspended in 70 percent ethanol in PBS and stored at 4°C until analysis. Prior to analysis, fixed cells were stained in a solution of propidium iodide in PBS with RNase A at 37 degrees for a minimum of 30 minutes. Cells were then strained and analyzed on a BD Accuri C6 benchtop flow cytometer (BD). Three proliferating samples of each genotype were analyzed and 20,000-50,000 cells were counted for each sample. Analysis shown in 7A was completed using FlowJo software (TreeStar).

### **Kinase Assays**

Cells were harvested in RIPA and lysed. Proliferating cells were harvested between 50 and 75 percent confluence and synchronized cells were serum-starved for 24 hours and then harvested at two-hour intervals following release into the cell cycle. Cell lysates were incubated in cyclin E antibody overnight on a rotator at 4 degrees Celsius. The next morning, sepharose beads were added to the lysates and they were incubated for an additional hour and a half at room temperature. Beads were precipitated on ice and the supernatant was removed, followed by two washes with RIPA and two washed with histone wash buffer (25mM Tris-HCl pH 7.5, 70mM NaCl, 10mM MgCl<sub>2</sub>, 1mM dithiothreitol). Kinase reactions were then completed in the microcentrifuge tubes containing the kinase and beads according to the protocol provided with the Universal Kinase Activity Kit (R&D Systems, product number EA004). Following the final incubation, the liquid contents of each tube were transferred to a 96 well plate and the absorbance was read at 630nm on a BioTek Synergy HT plate reader. Data was analyzed using Microsoft Excel.

### Construction of cyclin E mutants

The majority of the alanine scanning mutants were a kind gift from Jim Roberts at the Fred Hutchinson Cancer Center (Kelly et al., 1998). The point mutants were made using site-directed mutagenesis and all point mutants were confirmed by sequencing. Alanine scanning mutants that demonstrated a phenotype were also re-confirmed by sequencing. Truncations were cloned by using mutagenesis to generate a stop codon at the designated location in the cyclin E protein. Both deletions were made using site-directed mutagenesis and were also confirmed by sequencing. Forward primer sequences for mutagenesis are as follows: Cyclin E  $\Delta$  2-86 5'-GGACTTGAATTCATGGTTTACCCAAACTCAA, Cyclin E KIDR point mutant (K48R) 5' -CGCCGTCCTGTCGATTCTGGCCATTTCTTCAT, Cyclin E $\Delta$ 31-82 5'-GCTCGCTCCAGGAAGGATGACCGGGTTTAC. Primer sequences for the cyclin E truncations are as follows: Cyclin E STOP 200 5'-TCATCTTTATTTATTTGAGCCAAACTTGAGGAA, and STOP 300 5'-TTTCCTTATGGTATATGAGCTGCTTCGGCCTGG. All reverse primers were reverse complements of the forward primers. The control YFP fusion protein construct was made by cloning YFP in frame with a Flag tag into the pCMV-3Tag-6 vector. The cyclin E-YFP fusion was then constructed by cloning residues 2 through 86 of cyclin E in between the Flag-tag and YFP.

### Chou-Fasman Structure prediction

The Chou-Fasman algorithm was used for the structural prediction shown in Figure 6C (Chou and Fasman, 1975).

**List of Abbreviations:**

BTB: Bric-a-brac, Tramtrack, Broad-Complex

HSF2: Heat Shock Factor 2

KO: (Cul3) Knock Out

MEF: Mouse Embryonic Fibroblasts

MT: Myc-tagged

LMW cyclin E: Low Molecular Weight cyclin E

SCF: Skp1, Cul1, Fbxw7

WT: Wild-type

**Declarations:**

**Ethics approval and consent to participate:** Not applicable

**Consent for Publication:** Not applicable

**Availability of Data and Material:** Not applicable

**Declaration of Interests:**

The authors declare no competing interests.

**Funding:**

This work was supported by RO1 R01DK051496 (sub award to JDS).

**Authors' Contributions:**

BD wrote the manuscript and performed experiments shown in Figures 1 through 7 and S3. JDS performed experiments shown in Figures 4B, 7C, S1 and S5, edited the manuscript, conceived of the project and supervised the work. KR conducted the experiments shown in Figures 3C and S4. NLA and CDS provided the Cul3 KO 293 cells.

**Acknowledgements:**

The authors would like to thank the other members of the Singer lab at Portland State University, the Sigma-Xi chapter at Portland State and the members of the Ellison and McCormick labs at Oregon Health and Science University for worthwhile discussions. Lastly, the authors would like to thank Dr. James Roberts for the kind gift of the cyclin E linker scanning mutants utilized in this study and Shaun Debow for assistance with the ubiquitin mutants shown in figure S3.



## References:

- AKLI, S., BUI, T., WINGATE, H., BIERNACKA, A., MOULDER, S., TUCKER, S. L., HUNT, K. K. & KEYOMARSI, K. 2010. Low-molecular-weight cyclin E can bypass letrozole-induced G1 arrest in human breast cancer cells and tumors. *Clin Cancer Res*, 16, 1179-90.
- AKLI, S., ZHENG, P. J., MULTANI, A. S., WINGATE, H. F., PATHAK, S., ZHANG, N., TUCKER, S. L., CHANG, S. & KEYOMARSI, K. 2004. Tumor-specific low molecular weight forms of cyclin E induce genomic instability and resistance to p21, p27, and antiestrogens in breast cancer. *Cancer Res*, 64, 3198-208.
- BAGHERI-YARMAND, R., BIERNACKA, A., HUNT, K. K. & KEYOMARSI, K. 2010. Low molecular weight cyclin E overexpression shortens mitosis, leading to chromosome missegregation and centrosome amplification. *Cancer Res*, 70, 5074-84.
- BHASKARAN, N., VAN DROGEN, F., NG, H. F., KUMAR, R., EKHOLM-REED, S., PETER, M., SANGFELT, O. & REED, S. I. 2013. Fbw7alpha and Fbw7gamma collaborate to shuttle cyclin E1 into the nucleolus for multiubiquitylation. *Mol Cell Biol*, 33, 85-97.
- BOYDEN, L. M., CHOI, M., CHOATE, K. A., NELSON-WILLIAMS, C. J., FARHI, A., TOKA, H. R., TIKHONOVA, I. R., BJORNSEN, R., GHARAVI, A. G., GOILAV, B. & LIFTON, R. P. 2012. Mutations in kelch-like 3 and cullin 3 cause hypertension and electrolyte abnormalities. *Nature Genetics*, 1-11.
- CHEN, Y., YANG, Z., MENG, M., ZHAO, Y., DONG, N., YAN, H., LIU, L., DING, M., PENG, H. B. & SHAO, F. 2009. Cullin mediates degradation of RhoA through evolutionarily conserved BTB adaptors to control actin cytoskeleton structure and cell movement. *Mol Cell*, 35, 841-55.
- CHOI, Y. M., KIM, K. B., LEE, J. H., CHUN, Y. K., AN, I. S., AN, S. & BAE, S. 2016. DBC2/RhoBTB2 functions as a tumor suppressor protein via Musashi-2 ubiquitination in breast cancer. *Oncogene*.
- CHOU, P. Y. & FASMAN, G. D. 1975. The conformation of glucagon: predictions and consequences. *Biochemistry*, 14, 2536-41.
- CLURMAN, B. E., SHEAFF, R. J., THRESS, K., GROUDINE, M. & ROBERTS, J. M. 1996. Turnover of cyclin E by the ubiquitin-proteasome pathway is regulated by cdk2 binding and cyclin phosphorylation. *Genes Dev*, 10, 1979-90.
- CUMMINGS, C. M., BENTLEY, C. A., PERDUE, S. A., BAAS, P. W. & SINGER, J. D. 2009. The Cul3/Klhdhc5 E3 ligase regulates p60/katanin and is required for normal mitosis in mammalian cells. *J Biol Chem*, 284, 11663-75.
- DELK, N. A., HUNT, K. K. & KEYOMARSI, K. 2009. Altered subcellular localization of tumor-specific cyclin E isoforms affects cyclin-dependent kinase 2 complex formation and proteasomal regulation. *Cancer Res*, 69, 2817-25.
- DUDA, D. M., BORG, L. A., SCOTT, D. C., HUNT, H. W., HAMMEL, M. & SCHULMAN, B. A. 2008. Structural insights into NEDD8 activation of cullin-RING ligases: conformational control of conjugation. *Cell*, 134, 995-1006.
- DUONG, M. T., AKLI, S., WEI, C., WINGATE, H. F., LIU, W., LU, Y., YI, M., MILLS, G. B., HUNT, K. K. & KEYOMARSI, K. 2012. LMW-E/CDK2 deregulates acinar morphogenesis, induces tumorigenesis, and associates with the activated b-Raf-ERK1/2-mTOR pathway in breast cancer patients. *PLoS Genet*, 8, e1002538.

- GENG, Y., YU, Q., SICINSKA, E., DAS, M., SCHNEIDER, J. E., BHATTACHARYA, S., RIDEOUT, W. M., BRONSON, R. T., GARDNER, H. & SICINSKI, P. 2003. Cyclin E ablation in the mouse. *Cell*, 114, 431-43.
- GEYER, R., WEE, S., ANDERSON, S., YATES, J. & WOLF, D. A. 2003. BTB/POZ domain proteins are putative substrate adaptors for cullin 3 ubiquitin ligases. *Mol Cell*, 12, 783-90.
- HAO, B., OEHLMANN, S., SOWA, M. E., HARPER, J. W. & PAVLETICH, N. P. 2007. Structure of a Fbw7-Skp1-cyclin E complex: multisite-phosphorylated substrate recognition by SCF ubiquitin ligases. *Mol Cell*, 26, 131-43.
- HARWELL, R. M., PORTER, D. C., DANES, C. & KEYOMARSI, K. 2000. Processing of cyclin E differs between normal and tumor breast cells. *Cancer Res*, 60, 481-9.
- HONDA, R., LOWE, E. D., DUBININA, E., SKAMNAKI, V., COOK, A., BROWN, N. R. & JOHNSON, L. N. 2005. The structure of cyclin E1/CDK2: implications for CDK2 activation and CDK2-independent roles. *EMBO J*, 24, 452-63.
- IBEAUWUCHI, S. R., AGBOR, L. N., QUELLE, F. W. & SIGMUND, C. D. 2015. Hypertension-causing Mutations in Cullin3 Protein Impair RhoA Protein Ubiquitination and Augment the Association with Substrate Adaptors. *J Biol Chem*, 290, 19208-17.
- JIN, J. & HARPER, J. W. 2002. RING finger specificity in SCF-driven protein destruction. *Dev Cell*, 2, 685-7.
- KELLY, B. L., WOLFE, K. G. & ROBERTS, J. M. 1998. Identification of a substrate-targeting domain in cyclin E necessary for phosphorylation of the retinoblastoma protein. *Proc Natl Acad Sci U S A*, 95, 2535-40.
- KEYOMARSI, K., CONTE, D., JR., TOYOFUKU, W. & FOX, M. P. 1995. Dereglulation of cyclin E in breast cancer. *Oncogene*, 11, 941-50.
- KOEPP, D. M., SCHAEFER, L. K., YE, X., KEYOMARSI, K., CHU, C., HARPER, J. W. & ELLEDGE, S. J. 2001. Phosphorylation-dependent ubiquitination of cyclin E by the SCFFbw7 ubiquitin ligase. *Science*, 294, 173-7.
- KOFF, A., CROSS, F., FISHER, A., SCHUMACHER, J., LEGUELLEC, K., PHILIPPE, M. & ROBERTS, J. M. 1991. Human cyclin E, a new cyclin that interacts with two members of the CDC2 gene family. *Cell*, 66, 1217-28.
- KWON, J. E., LA, M., OH, K. H., OH, Y. M., KIM, G. R., SEOL, J. H., BAEK, S. H., CHIBA, T., TANAKA, K., BANG, O. S., JOE, C. O. & CHUNG, C. H. 2006. BTB domain-containing speckle-type POZ protein (SPOP) serves as an adaptor of Daxx for ubiquitination by Cul3-based ubiquitin ligase. *J Biol Chem*, 281, 12664-72.
- LANEY, J. D. & HOCHSTRASSER, M. 1999. Substrate targeting in the ubiquitin system. *Cell*, 97, 427-30.
- LEW, D. J., DULIC, V. & REED, S. I. 1991. Isolation of three novel human cyclins by rescue of G1 cyclin (Cln) function in yeast. *Cell*, 66, 1197-206.
- LIBERTINI, S. J., ROBINSON, B. S., DHILLON, N. K., GLICK, D., GEORGE, M., DANDEKAR, S., GREGG, J. P., SAWAI, E. & MUDRYJ, M. 2005. Cyclin E both regulates and is regulated by calpain 2, a protease associated with metastatic breast cancer phenotype. *Cancer Res*, 65, 10700-8.
- LOEB, K. R., KOSTNER, H., FIRPO, E., NORWOOD, T., TSUCHIYA, K. D., CLURMAN, B. E. & ROBERTS, J. M. 2005. A mouse model for cyclin E-dependent genetic instability and tumorigenesis. *Cancer Cell*, 8, 35-47.
- LU, A. & PFEFFER, S. R. 2013. Golgi-associated RhoBTB3 targets cyclin E for ubiquitylation and promotes cell cycle progression. *J Cell Biol*, 203, 233-50.
- MCCORMICK, J. A., YANG, C. L., ZHANG, C., DAVIDGE, B., BLANKENSTEIN, K. I., TERKER, A. S., YARBROUGH, B., MEERMEIER, N. P., PARK, H. J., MCCULLY, B., WEST, M.,

- BORSCHESKI, A., HIMMERKUS, N., BLEICH, M., BACHMANN, S., MUTIG, K., ARGALIZ, E. R., GAMBA, G., SINGER, J. D. & ELLISON, D. H. 2014. Hyperkalemic hypertension-associated cullin 3 promotes WNK signaling by degrading KLHL3. *J Clin Invest*, 124, 4723-36.
- MCEVOY, J., KOSSATZ, U., MALEK, N. & SINGER, J. 2007. Constitutive turnover of cyclin E by Cul3 maintains quiescence. *Molecular Cell Biology*, 27, 3651-66.
- MINELLA, A. C., LOEB, K. R., KNECHT, A., WELCKER, M., VARNUM-FINNEY, B. J., BERNSTEIN, I. D., ROBERTS, J. M. & CLURMAN, B. E. 2008. Cyclin E phosphorylation regulates cell proliferation in hematopoietic and epithelial lineages in vivo. *Genes Dev*, 22, 1677-89.
- PETROSKI, M. D. & DESHAIES, R. J. 2005. Function and regulation of cullin-RING ubiquitin ligases. *Nat Rev Mol Cell Biol*, 6, 9-20.
- PINTARD, L., WILLEMS, A. & PETER, M. 2004. Cullin-based ubiquitin ligases: Cul3-BTB complexes join the family. *EMBO J*, 23, 1681-7.
- PINTARD, L., WILLIS, J. H., WILLEMS, A., JOHNSON, J. L., SRAYKO, M., KURZ, T., GLASER, S., MAINS, P. E., TYERS, M., BOWERMAN, B. & PETER, M. 2003. The BTB protein MEL-26 is a substrate-specific adaptor of the CUL-3 ubiquitin-ligase. *Nature*, 425, 311-6.
- PORTER, D. C. & KEYOMARSI, K. 2000. Novel splice variants of cyclin E with altered substrate specificity. *Nucleic Acids Res*, 28, E101.
- PORTER, D. C., ZHANG, N., DANES, C., MCGAHREN, M. J., HARWELL, R. M., FARUKI, S. & KEYOMARSI, K. 2001. Tumor-specific proteolytic processing of cyclin E generates hyperactive lower-molecular-weight forms. *Mol Cell Biol*, 21, 6254-69.
- RAASI, S. & PICKART, C. M. 2005. Ubiquitin chain synthesis. *Methods Mol Biol*, 301, 47-55.
- RATH, S. L. & SENAPATI, S. 2014. Why are the truncated cyclin Es more effective CDK2 activators than the full-length isoforms? *Biochemistry*, 53, 4612-24.
- RICHARDSON, H. E., O'KEEFE, L. V., REED, S. I. & SAINT, R. 1993. A Drosophila G1-specific cyclin E homolog exhibits different modes of expression during embryogenesis. *Development*, 119, 673-90.
- ROGERS, S., WELLS, R. & RECHSTEINER, M. 1986. Amino acid sequences common to rapidly degraded proteins: the PEST hypothesis. *Science*, 234, 364-8.
- ROGERS, S. W. & RECHSTEINER, M. C. 1986. Microinjection studies on selective protein degradation: relationships between stability, structure, and location. *Biomed Biochim Acta*, 45, 1611-8.
- SAID, T. K. & MEDINA, D. 1995. Cell cyclins and cyclin-dependent kinase activities in mouse mammary tumor development. *Carcinogenesis*, 16, 823-30.
- SCUDERI, R., PALUCKA, K. A., POKROVSKAJA, K., BJORKHOLM, M., WIMAN, K. G. & PISA, P. 1996. Cyclin E overexpression in relapsed adult acute lymphoblastic leukemias of B-cell lineage. *Blood*, 87, 3360-7.
- SHERR, C. J. & ROBERTS, J. M. 1999. CDK inhibitors: positive and negative regulators of G1-phase progression. *Genes Dev*, 13, 1501-12.
- SINGER, J. D., GURIAN-WEST, M., CLURMAN, B. & ROBERTS, J. M. 1999. Cullin-3 targets cyclin E for ubiquitination and controls S phase in mammalian cells. *Genes Dev*, 13, 2375-87.
- STROHMAIER, H., SPRUCK, C. H., KAISER, P., WON, K. A., SANGFELT, O. & REED, S. I. 2001. Human F-box protein hCdc4 targets cyclin E for proteolysis and is mutated in a breast cancer cell line. *Nature*, 413, 316-22.
- TYERS, M. & JORGENSEN, P. 2000. Proteolysis and the cell cycle: with this RING I do thee destroy. *Curr Opin Genet Dev*, 10, 54-64.

- WANG, X. D., ROSALES, J. L., MAGLIOCCO, A., GNANAKUMAR, R. & LEE, K. Y. 2003. Cyclin E in breast tumors is cleaved into its low molecular weight forms by calpain. *Oncogene*, 22, 769-74.
- WELCKER, M., SINGER, J., LOEB, K. R., GRIM, J., BLOECHER, A., GURIEN-WEST, M., CLURMAN, B. E. & ROBERTS, J. M. 2003. Multisite phosphorylation by Cdk2 and GSK3 controls cyclin E degradation. *Mol Cell*, 12, 381-92.
- WIMUTTISUK, W. & SINGER, J. D. 2007. The Cullin3 ubiquitin ligase functions as a Nedd8-bound heterodimer. *Mol Biol Cell*, 18, 899-909.
- WIMUTTISUK, W., WEST, M., DAVIDGE, B., YU, K., SALOMON, A. & SINGER, J. D. 2014. Novel Cul3 binding proteins function to remodel E3 ligase complexes. *BMC Cell Biol*, 15, 28.
- WINGATE, H., ZHANG, N., MCGARHEN, M. J., BEDROSIAN, I., HARPER, J. W. & KEYOMARSI, K. 2005. The tumor-specific hyperactive forms of cyclin E are resistant to inhibition by p21 and p27. *J Biol Chem*, 280, 15148-57.
- XING, H., HONG, Y. & SARGE, K. D. 2010. PEST sequences mediate heat shock factor 2 turnover by interacting with the Cul3 subunit of the Cul3-RING ubiquitin ligase. *Cell Stress Chaperones*, 15, 301-8.
- ZARIWALA, M., LIU, J. & XIONG, Y. 1998. Cyclin E2, a novel human G1 cyclin and activating partner of CDK2 and CDK3, is induced by viral oncoproteins. *Oncogene*, 17, 2787-98.
- ZHANG, D. D., LO, S. C., CROSS, J. V., TEMPLETON, D. J. & HANNINK, M. 2004. Keap1 is a redox-regulated substrate adaptor protein for a Cul3-dependent ubiquitin ligase complex. *Mol Cell Biol*, 24, 10941-53.
- ZHANG, P., GAO, K., TANG, Y., JIN, X., AN, J., YU, H., WANG, H., ZHANG, Y., WANG, D., HUANG, H., YU, L. & WANG, C. 2014. Destruction of DDIT3/CHOP protein by wild-type SPOP but not prostate cancer-associated mutants. *Hum Mutat*.
- ZHENG, N., SCHULMAN, B. A., SONG, L., MILLER, J. J., JEFFREY, P. D., WANG, P., CHU, C., KOEPP, D. M., ELLEDGE, S. J., PAGANO, M., CONAWAY, R. C., CONAWAY, J. W., HARPER, J. W. & PAVLETICH, N. P. 2002. Structure of the Cul1-Rbx1-Skp1-F boxSkp2 SCF ubiquitin ligase complex. *Nature*, 416, 703-9.

# Figures

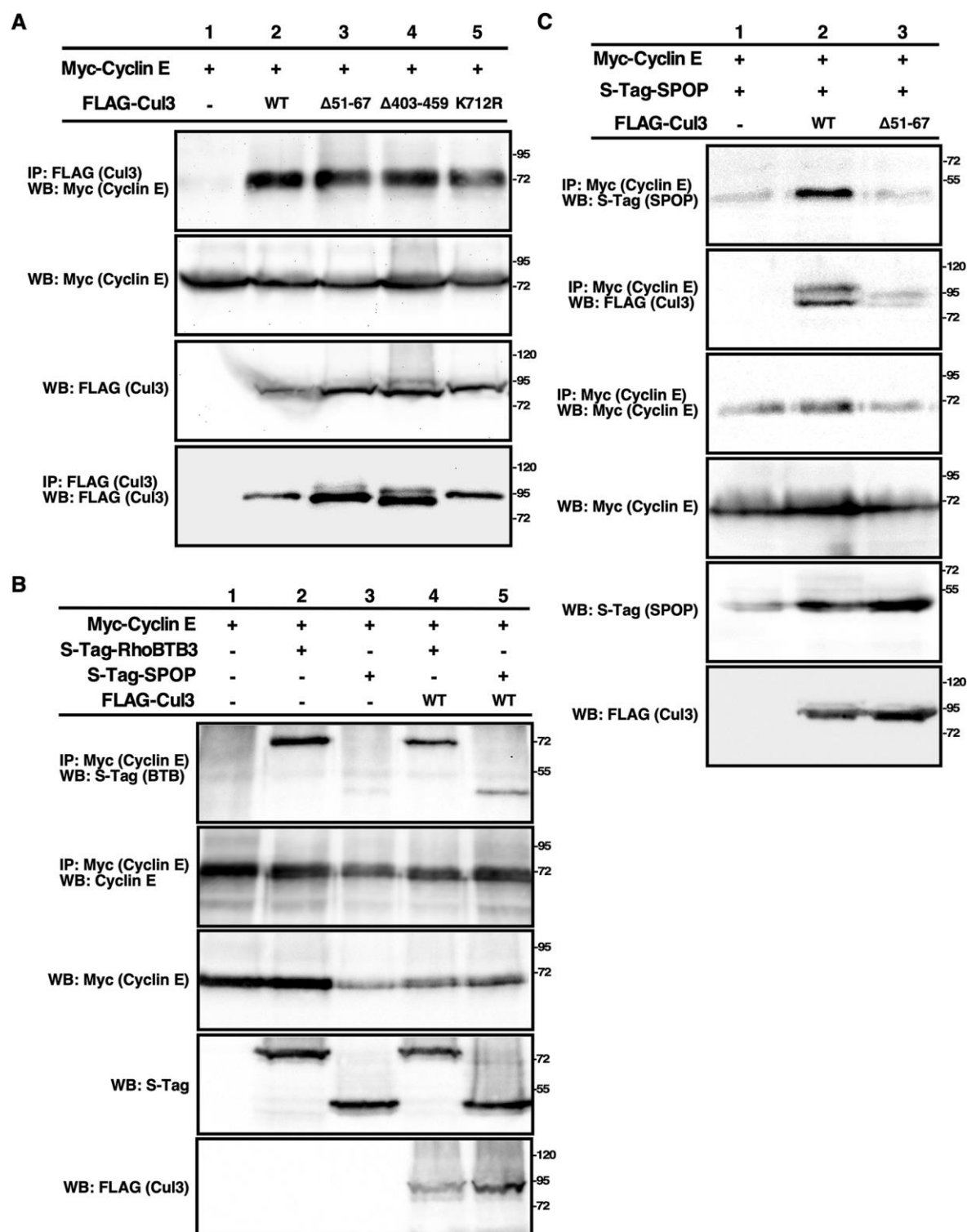


**Figure 1:** *Cul3 directly binds cyclin E.* A: HEK293 cells were co-transfected with Myc-cyclin E1 and different Flag-tagged Cul3 mutants including Cul3 $\Delta$ 51-67, Cul3 $\Delta$ 403-459, and Cul3K712R. Immunoprecipitations (IPs) were performed using a Flag antibody. A western blot using cyclin E antibody was performed to detect transfected cyclin E (top panel). B: Myc-cyclin E was co-transfected with S-RhoBTB3 (lanes 2 and 4) or S-SPOP (lanes 3 and 5), with Flag-Cul3 in lanes 4 and 5. IPs were performed using a polyclonal Myc antibody. IP results are shown in the top panel. The lower three panels show the original protein levels in the lysates. C: Flag-Cul3 or Flag-Cul3  $\Delta$ 51-67 was co-transfected with Myc-cyclin E, HA-ubiquitin, and S-tagged-SPOP. An IP for Myc-cyclin E was performed followed by western blotting to detect S-SPOP (C, top panel) and Flag-Cul3 (C, second panel). The lower three panels show the original protein levels of the lysates prior to immunoprecipitation. For all westerns, the migration of size markers is indicated on the sides of the gel images (kDa).



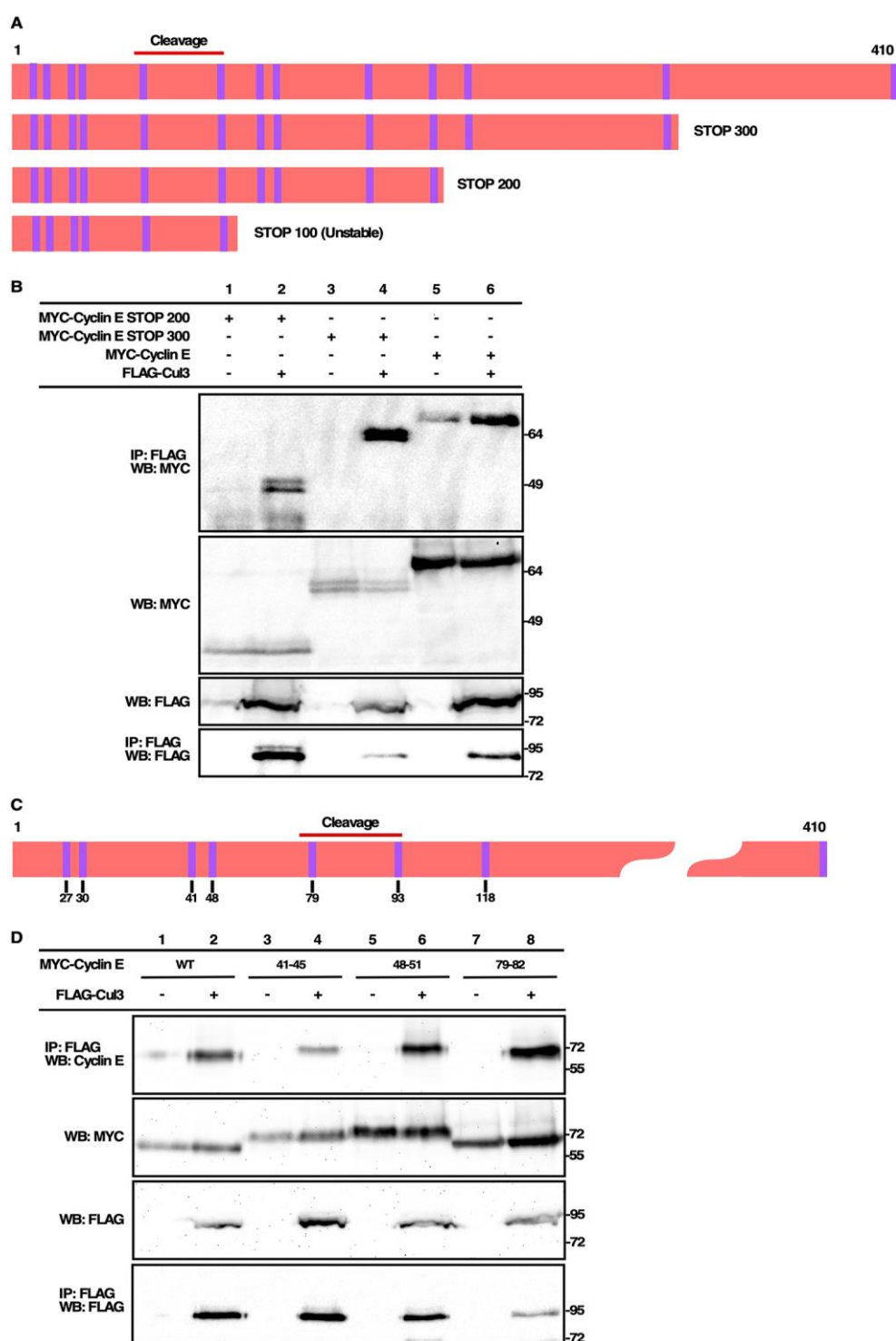


**Figure 2:** *The N-terminal domain of cyclin E is required for binding to Cul3.* A: A cartoon showing full length, wild-type cyclin E (top) and three truncation mutants throughout the protein, STOP100, STOP200, and STOP300. B: Upper blot, immunoprecipitation (IP) for

Flag-Cul3 and blot for Myc-cyclin E showing binding. Middle and middle blots show relative levels of transfected protein in cell extracts and the lower panel shows the Flag blot of the Flag IP. C: Cartoon depicting the locations of point mutants and alanine scanning mutants (designated here by the first mutated amino acid number) on cyclin E. The cleavage site which produces LMW cyclin E is shown in red. D: Upper blot, IP for Flag-Cul3 and western blot for Myc-cyclin E showing binding of three N-terminally located alanine scanning mutants (lanes 4, 6, and 8) in comparison to wild-type cyclin E (lane 2). The middle two blots show levels of transfected protein in the cell extracts. The lower panel shows the Flag blot of the flag IP. For all westerns, the migration of size markers is indicated on the sides of the gel images (kDa).



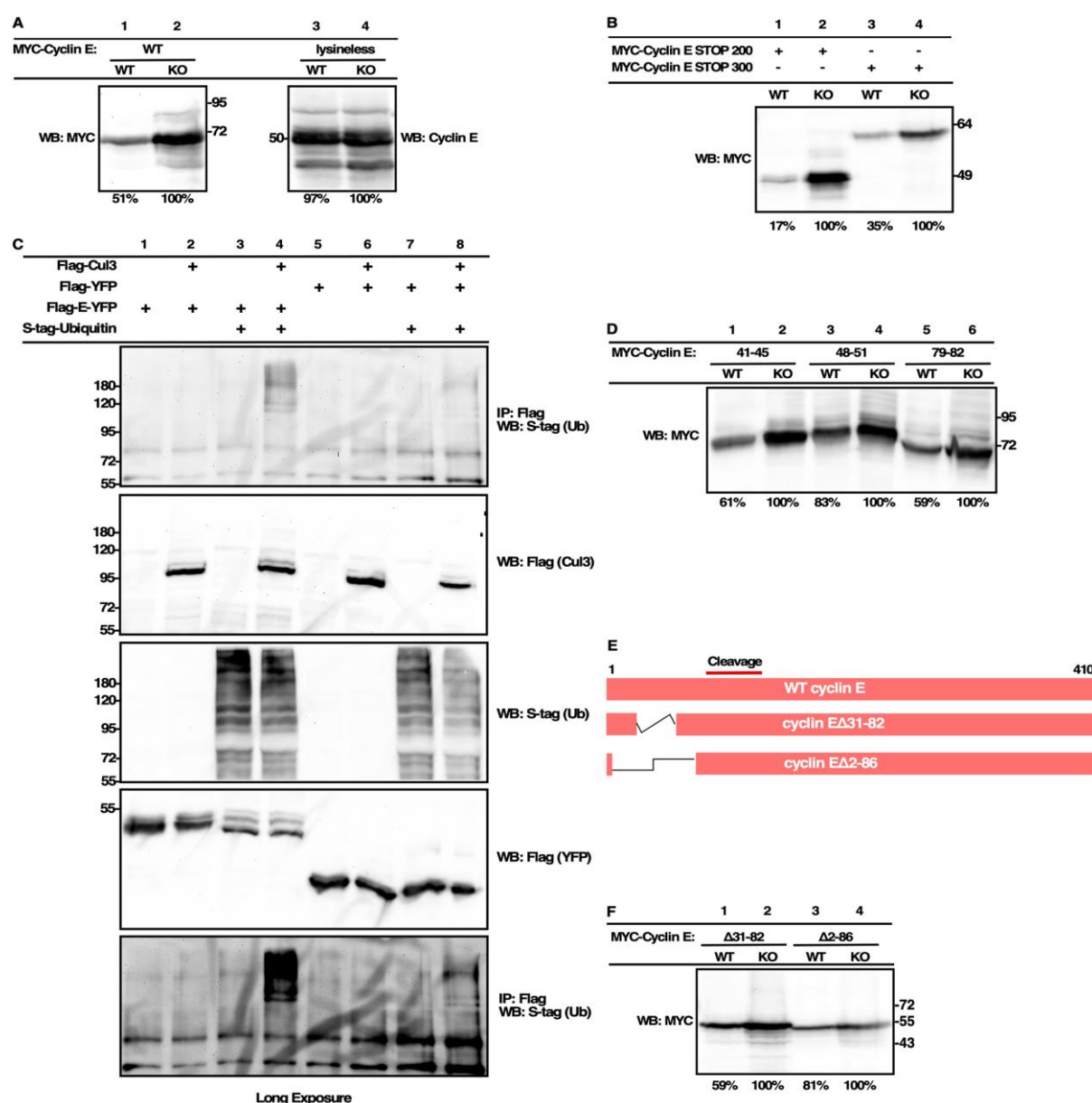


**Figure 3:** *The cyclin E N-terminal domain regulates cyclin E stability in the presence of Cul3.*

A: Cyclin E levels are shown when transfected into Cul3 KO cells when compared to WT 293 cells (A: Left panel). Lysineless cyclin E, which cannot be ubiquitinated, is shown in the right panel (A: Right panel). B: Myc-tagged STOP 200 and STOP 300 truncations of cyclin E were transfected into wild-type and Cul3 KO 293 cells and their expression was measured using a Myc (cyclin E) antibody. C: Ubiquitination assay showing the cyclin E residues 2-86 and YFP

fusion protein. Cells were transfected with either Flag-tagged cyclin E-YFP or Flag-tagged YFP in the presence and absence of ubiquitin and Cul3. Lysates were harvested and analyzed via IP (Flag) and western blot. Top panel: Results of the ubiquitination assay. The cyclin E-YFP fusion protein is shown in lanes 1 through 4 and wild-type YFP is shown in lanes 5 through 8. Middle panels: Western blots showing the total amount of protein in each lysate prior to the IPs. Lower panel: long exposure of the ubiquitination assay. D: Three Myc-tagged alanine scanning mutants, DPDEE→AAAAA (residues 41-45, lanes 1 and 2), KIDR→AIAA (amino acids 48-51, lanes 3 and 4) and DKED→AAAA (amino acids 79-82, lanes 5 and 6), were transfected into both WT and Cul3 KO cells and their abundance was measured using a Myc (cyclin E) antibody. E: Diagram showing two mutants in which portions of the N-terminal domain have been deleted. F: Expression of transfected Myc-cyclin E $\Delta$ 31-82 and Myc-cyclin E $\Delta$ 2-86 are shown in both the WT and KO cells (E, right panel, lanes 1 through 4). Quantification of each western blot (WB) is listed below each lane as a percent relative to the sample in the KO lane for each pair. For all westerns, the migration of size markers is indicated on the sides of the gel images (kDa).

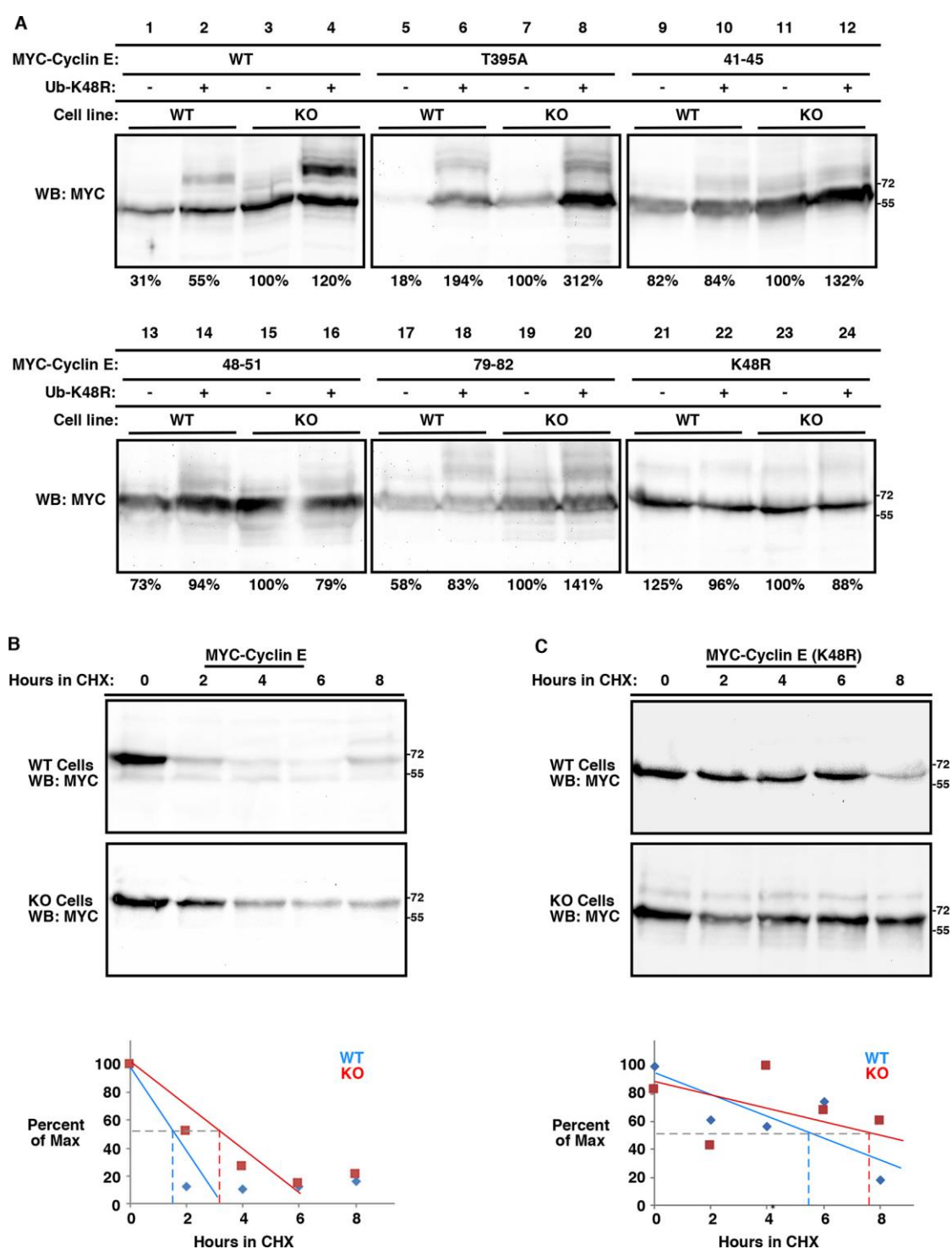


**Figure 4:** *Cul3-mediated ubiquitination of cyclin E on K48 regulates cyclin E abundance.* A: Alanine scanning and point mutants located within the first 200 amino acids of the cyclin E protein were transfected in WT and KO 293 cells in the presence or absence of an S-tagged

K48R ubiquitin construct. Wild-type cyclin E (lanes 1-4) and cyclin E T395A, which cannot be degraded by Cul1 (lanes 5-8), were included as controls. Three cyclin E alanine scanning mutants are shown here, DPDEE→AAAAA (residues 41-45, lanes 9-12), KIDR→AIAA (residues 48-51, lanes 13-16), and DKED→AAAA (residues 79-82, lanes 17-20). The point mutant cyclin E K48R is also shown (lanes 21-24). The total amount of protein in each lane was quantified. B and C: Cul3 WT and KO 293 cells were transfected with Myc-tagged cyclin E (B) or Myc-tagged cyclin EK48R (C). After 24 hours, cycloheximide was added and cells were harvested at the indicated time points. Half-lives were determined via Western blots (top), and quantified (bottom). For all westerns, the migration of size markers is indicated on the sides of the gel images (kDa).

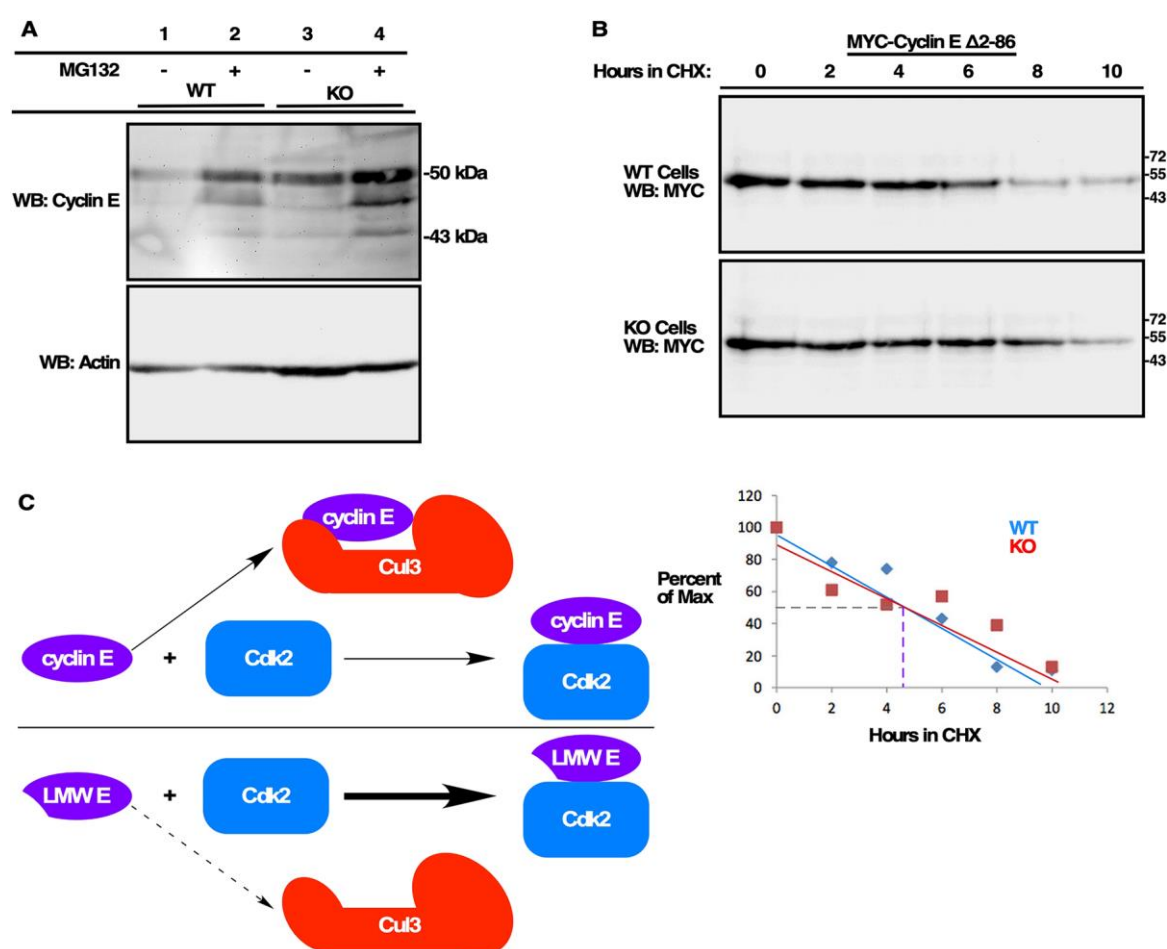


**Figure 5:** *LMW cyclin E is not degraded by Cul3.* A. The upper blot shows levels of endogenous cyclin E in WT and Cul3 KO 293 cells. The proteasome inhibitor MG132 has been added to the cells shown in lanes 2 and 4. The lower blot shows levels of actin in the same cells. B: WT and Cul3 KO 293 cells were transfected with cyclin EΔ2-86. Cycloheximide was added 24 hours post-transfection and cells were harvested every two hours following cycloheximide addition. Top panel: Western blots showing protein levels. Lower panel: quantification of results. C: Model showing full length cyclin E being ubiquitinated and degraded via Cul3 during G<sub>1</sub>, leaving some cyclin E available to activate Cdk2 (top). In cells containing LMW cyclin E lacking its N-terminal domain, proper ubiquitination by Cul3

might not occur, possibly contributing to increased activation of Cdk2. For all westerns, the migration of size markers is indicated on the sides of the gel images (kDa).



and 4) HEK 293 cells. E: Myc-tagged wild-type cyclin E1 (lanes 1 and 2), the 48-51 (KIDR) alanine scanning mutant (lanes 3 and 4), and Myc-cyclin E2 (lanes 5 and 6) were transfected in the presence and absence of Flag-Cul3 and immunoprecipitated using a Flag antibody. Upper blot: Flag IP, Myc western blot showing the IP results. Lower blots: Western blots showing protein expression levels. For all westerns, the migration of size markers is indicated on the sides of the gel images (kDa).



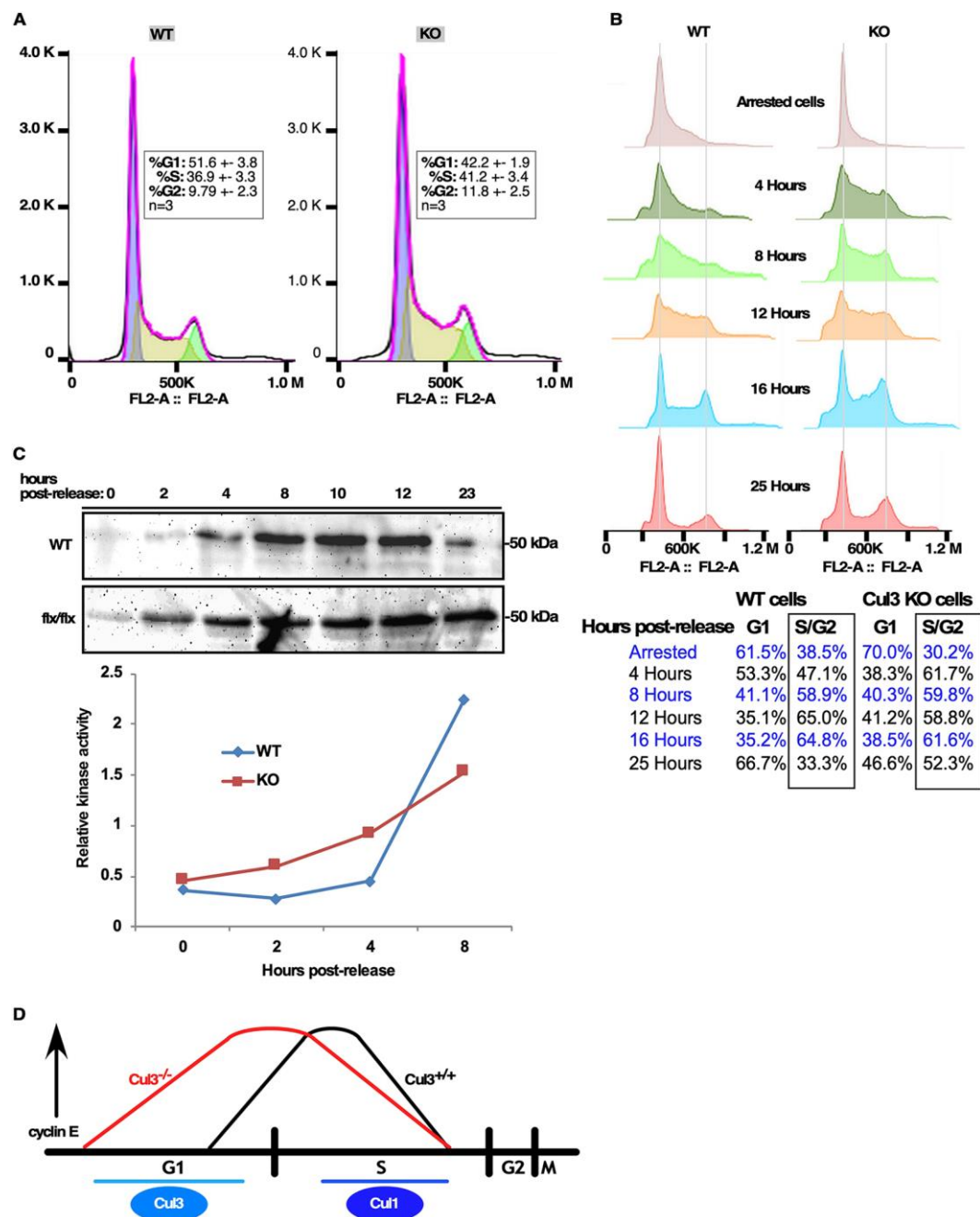


**Figure 7:** *Cul3 regulates cyclin E degradation early during G<sub>1</sub>.* A: Flow cytometry analysis of proliferating 293 cells. WT cells are shown on the left and Cul3 KO cells are shown on the right. Cells in G<sub>1</sub> are shown in purple, S-phase cells are shown in yellow, and G<sub>2</sub>/M cells are shown in green. The quantification shown represents the mean of three experiments. B: Cells were serum-starved and released into G<sub>1</sub>. Cells were harvested at 4-hour intervals, stained with

propidium iodide, and analyzed by flow cytometry. C: Western blot showing levels of endogenous cyclin E in mouse embryonic fibroblasts (MEFs) that are wild-type (WT, western blot, top row) or deficient for Cul3 (flx/flx, western blot, bottom row). Results of a kinase assay for cyclin E/Cdk2 activity in synchronized 293 cells are shown in the graph beneath the western blot. Cells were synchronized in G1 and then released and harvested at the indicated time points. Cyclin E and Cdk2 were purified from the lysates via immunoprecipitation and then used in a kinase assay which couples kinase activity to phosphate production (Graph beneath western blots). Cells that had been serum-starved and released were collected at two-hour intervals as indicated. D: These data are consistent with a model where Cul3 is responsible for maintaining cyclin E levels during G<sub>1</sub> in order to prevent early entrance into S-phase. Cul1 is known to degrade cyclin E after S-phase has begun.

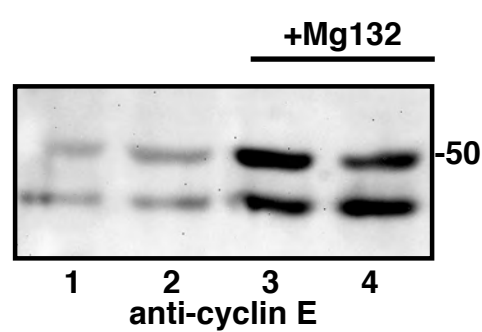


**Figure S1:** Transfected cyclin E is stabilized by MG132. WT 293 cells were transfected with wild-type myc-tagged cyclin E. MG132 was added 18 hours before harvest to the indicated samples. Cells were harvested, lysed and analyzed by western blot. Migration of size markers indicated to the right of gel image (kDa).

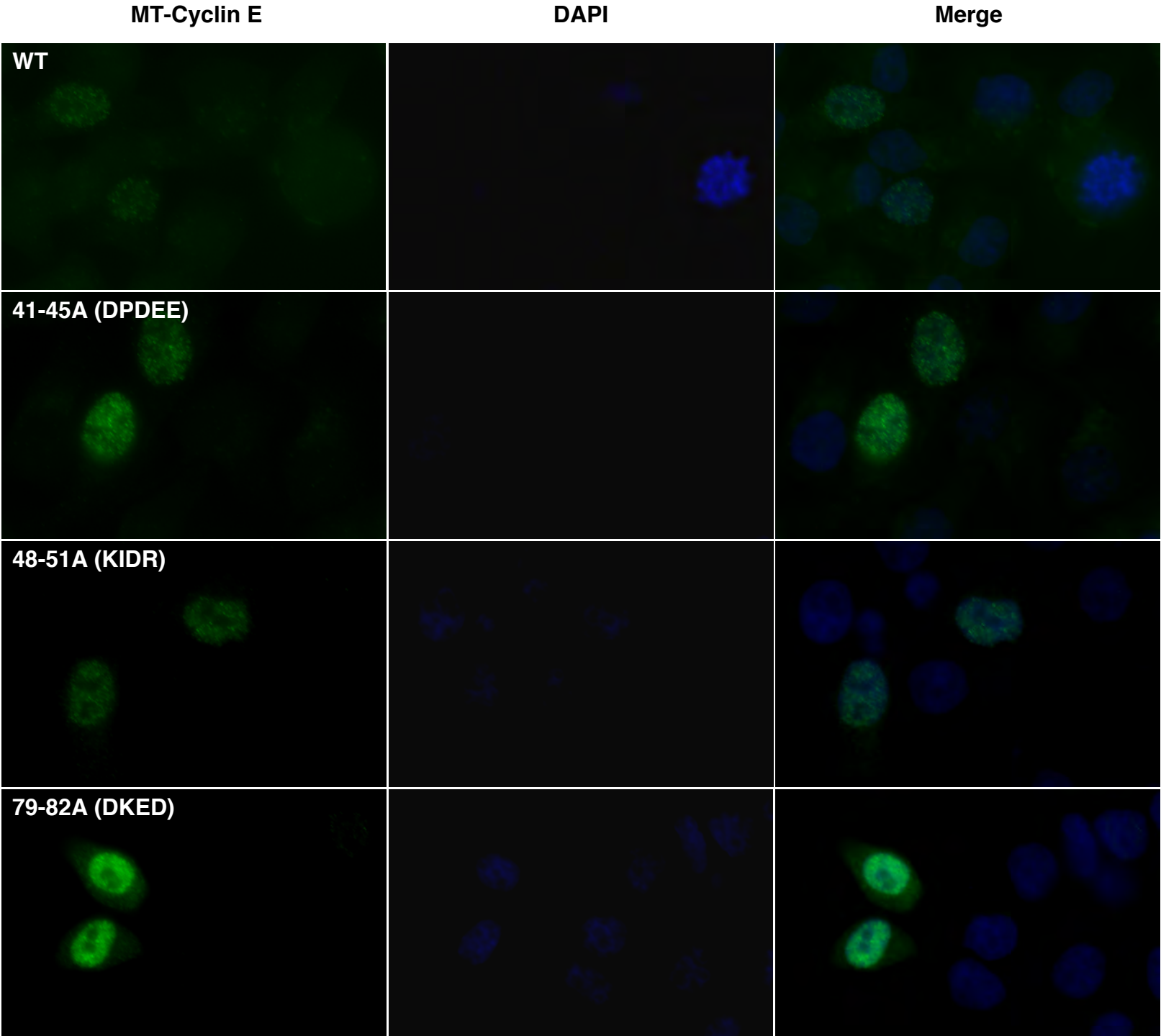


**Figure S2:** Localization of cyclin E mutants are the same as wild-type. Myc-tagged cyclin E mutants were transfected into HeLa cells and localization was determined using immunofluorescence. The localization of several mutants is shown: DPDEE (41-45)→AAAAA (row 2), KIDR (48-51)→AIAA (row 3), and DKED (97-82)→AAAA (row 4). The top row shows the localization of wild-type cyclin E.

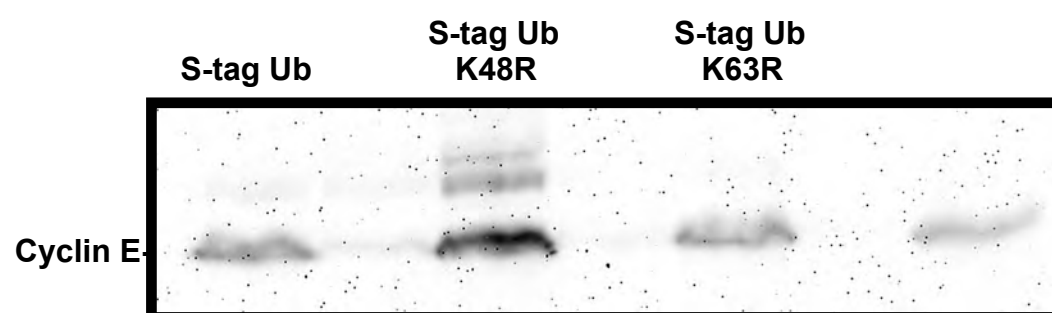
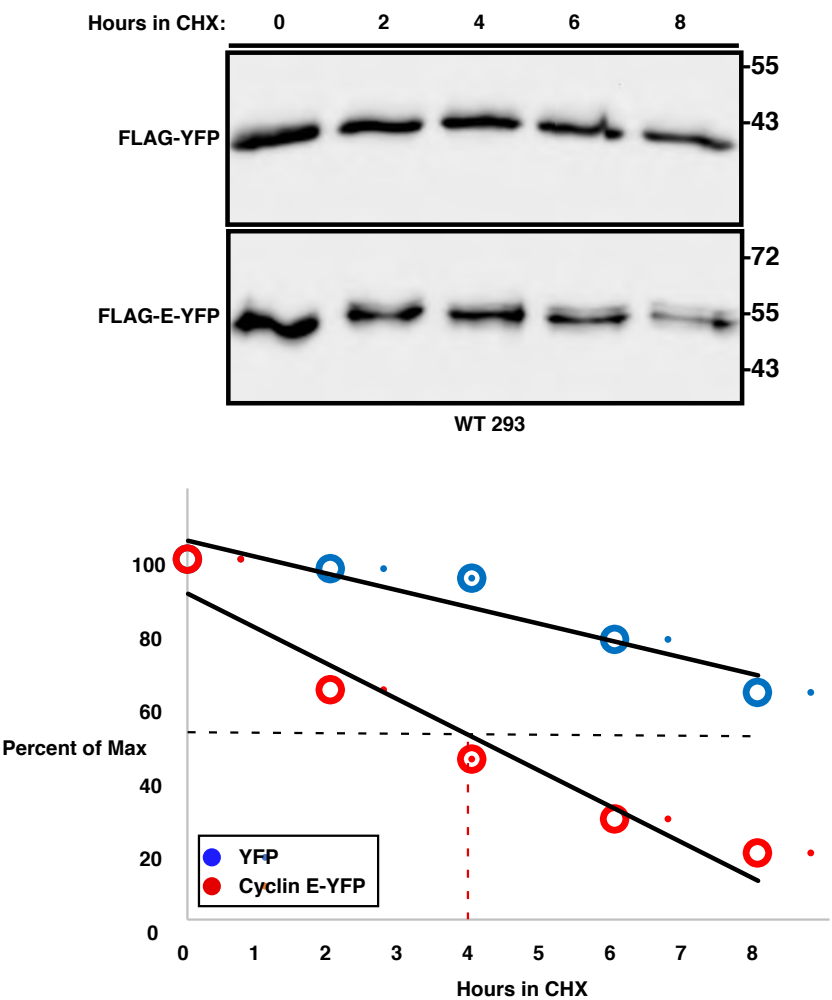


**Figure S3:** Ubiquitin mutants and cyclin E. Myc-cyclin E was transfected in the presence or absence of S-tagged ubiquitin mutants. The Ubiquitinmutant K48R, which cannot form degradative linkages is shown in lane 2. Ubiquitin mutant K63R, which cannot form non-degradative K63 linkages, is shown in lane 3. Cyclin E alone is shown in lanes 1 and 4.

A.



B.

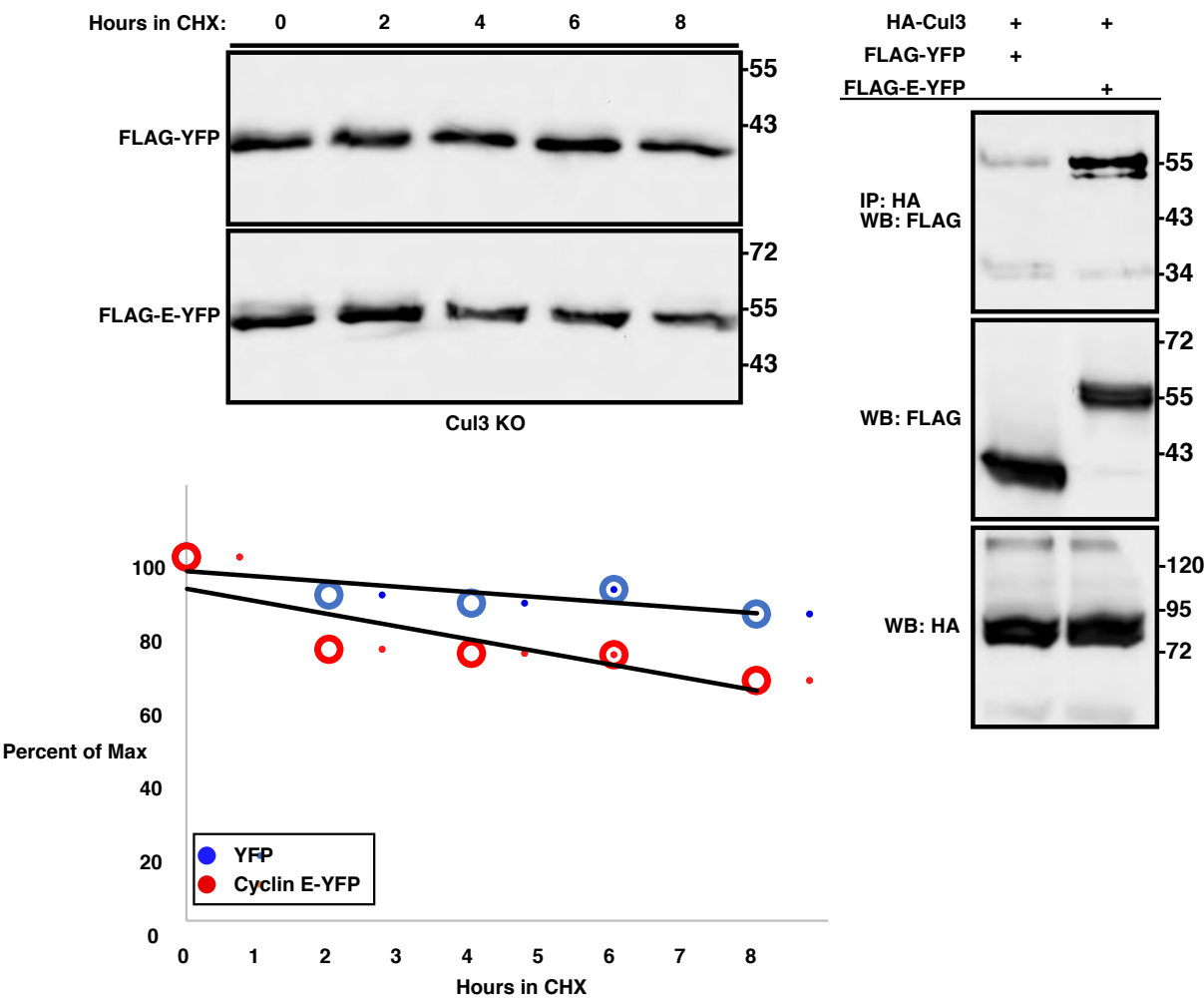


**Figure S4:** The cyclin E N-terminus induces degradation of a YFP fusion protein. A: Cyclin E residues 2 through 86 were fused to a Flag-tagged YFP construct. Half-lives of the resulting cyclin E-YFP fusion protein were then measured in 293 cells and compared to a Flag-tagged YFP control. The resulting western blots (top panel) were quantified and the half-life of the control YFP is shown in blue and cyclin E-YFP fusion protein is shown in red (graph, bottom panel). B: YFP (lane 1) or the cyclin E-YFP fusion protein (lane 2) were co-transfected with HA-tagged Cul3 and immunoprecipitated using HA antibody. IP results are shown in the top panel. The two lower panels show relative amounts of protein in each of the original samples. Migration of size markers indicated to the right of gel images (kDa).

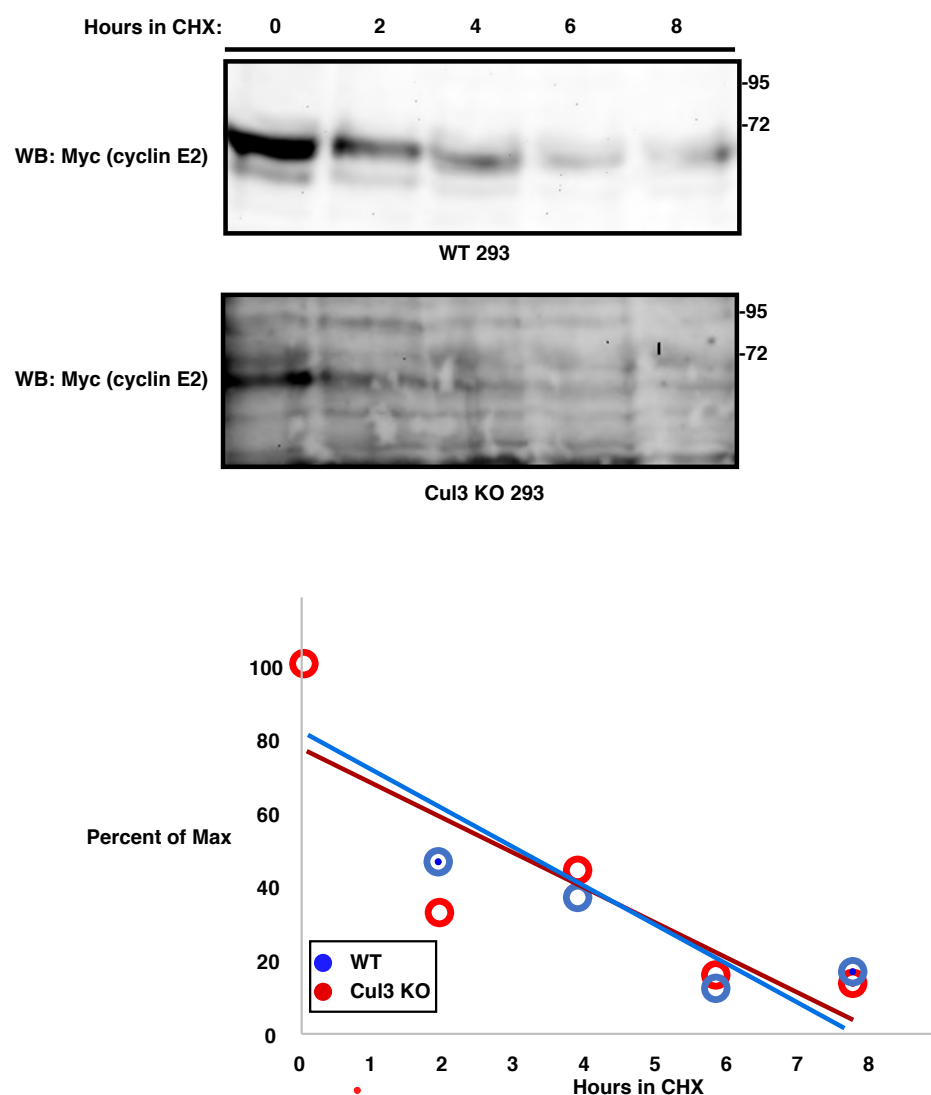


**Figure S5:** Cul3 has no effect on the half-life of cyclin E2. WT and Cul3KO 293 cells were transfected with Myc-cyclin E2. Cycloheximide was added 24 hours post-transfection and cells were harvested every two hours following cycloheximide addition. Top panel: Western blots showing protein expression levels. Migration of size markers indicated to the right of gel images (kDa). Lower panel: plot of half lives as percent of maximum signal.

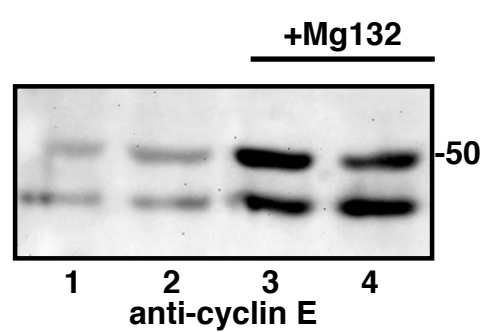


**Figure S1:** Transfected cyclin E is stabilized by MG132. WT 293 cells were transfected with wild-type myc-tagged cyclin E. MG132 was added 18 hours before harvest to the indicated samples. Cells were harvested, lysed and analyzed by western blot. Migration of size markers indicated to the right of gel image (kDa).



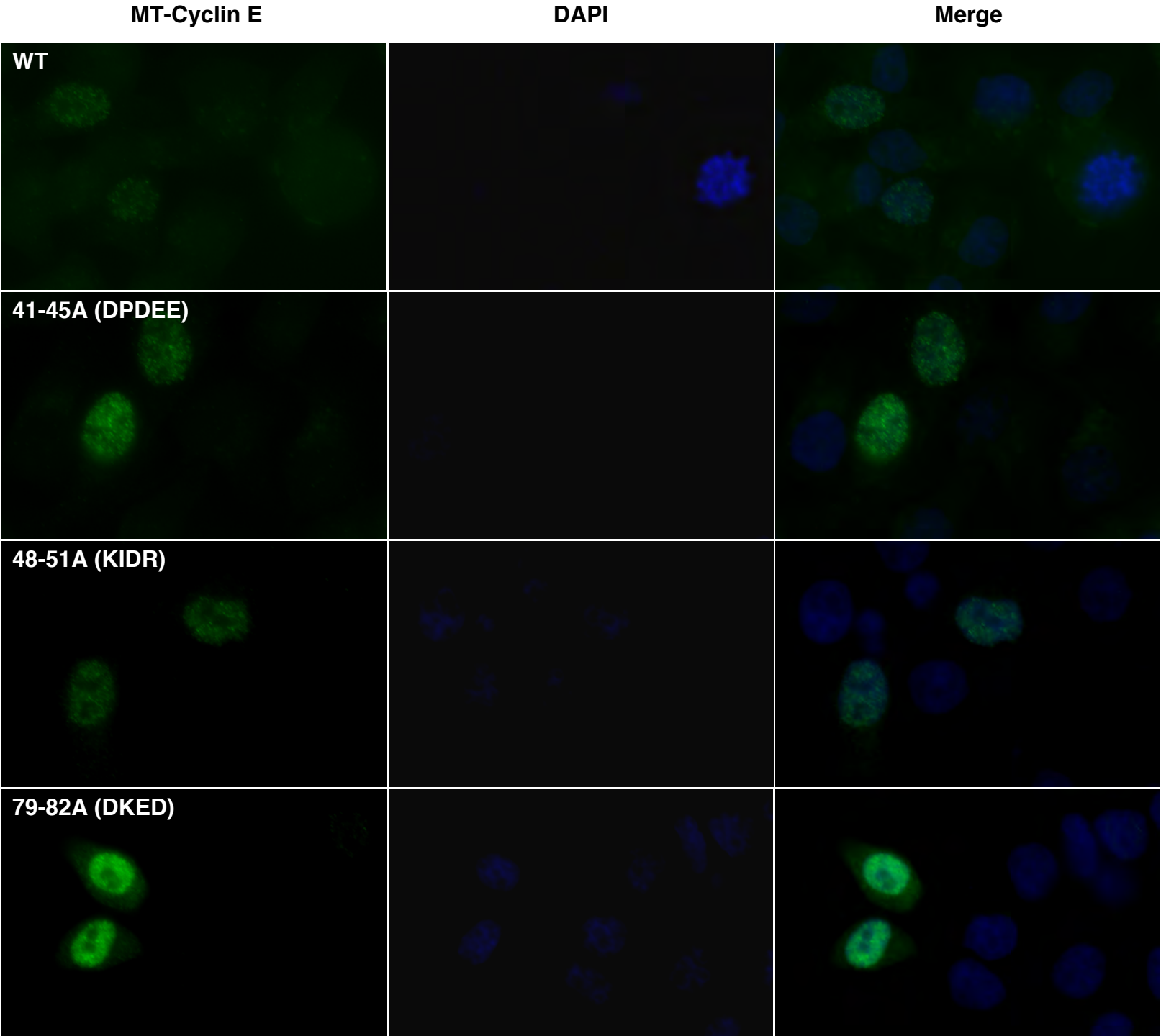


**Figure S2:** Localization of cyclin E mutants are the same as wild-type. Myc-tagged cyclin E mutants were transfected into HeLa cells and localization was determined using immunofluorescence. The localization of several mutants is shown: DPDEE (41-45)→AAAAA (row 2), KIDR (48-51)→AIAA (row 3), and DKED (97-82)→AAAA (row 4). The top row shows the localization of wild-type cyclin E.

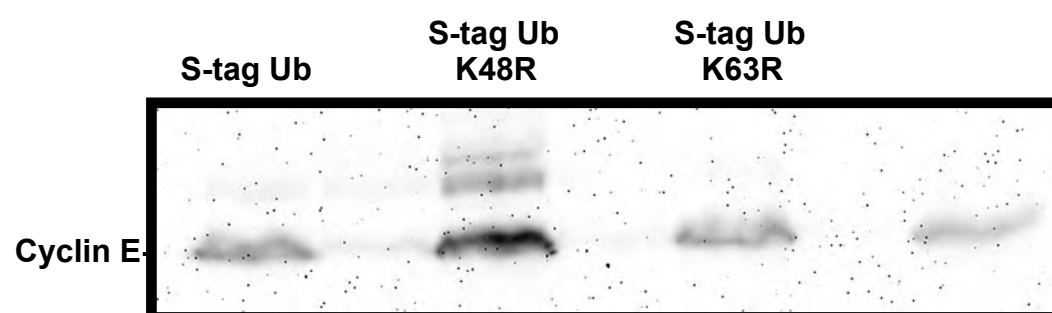
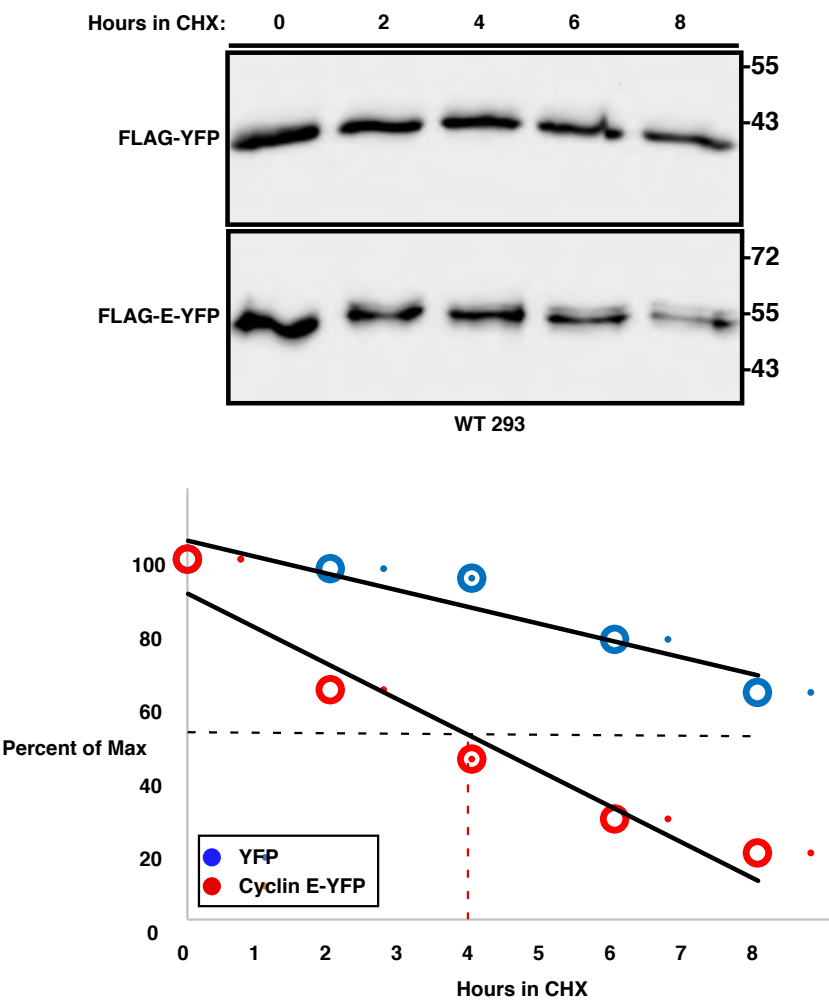


**Figure S3:** Ubiquitin mutants and cyclin E. Myc-cyclin E was transfected in the presence or absence of S-tagged ubiquitin mutants. The Ubiquitinmutant K48R, which cannot form degradative linkages is shown in lane 2. Ubiquitin mutant K63R, which cannot form non-degradative K63 linkages, is shown in lane 3. Cyclin E alone is shown in lanes 1 and 4.

A.



B.

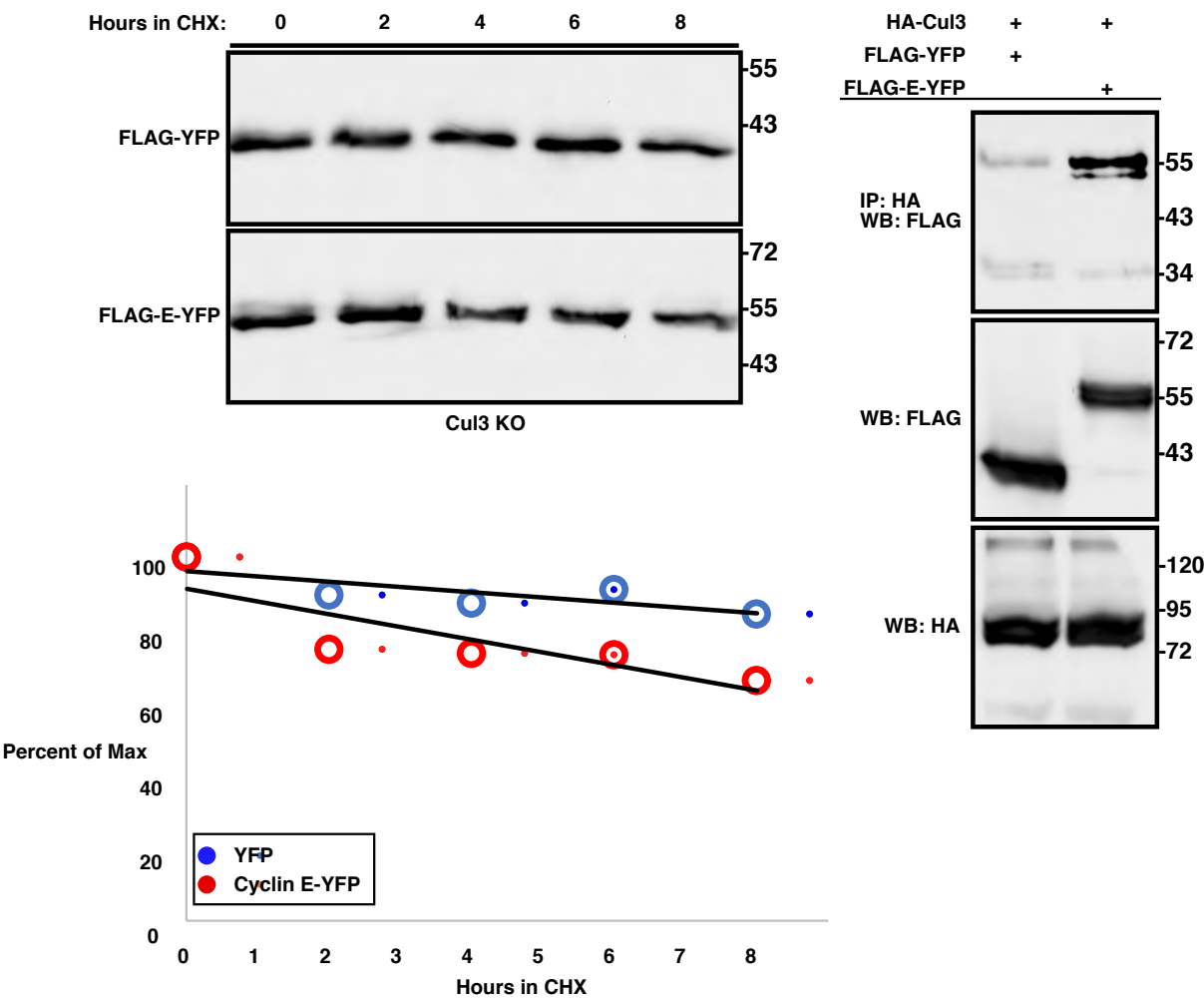


**Figure S4:** The cyclin E N-terminus induces degradation of a YFP fusion protein. A: Cyclin E residues 2 through 86 were fused to a Flag-tagged YFP construct. Half-lives of the resulting cyclin E-YFP fusion protein were then measured in 293 cells and compared to a Flag-tagged YFP control. The resulting western blots (top panel) were quantified and the half-life of the control YFP is shown in blue and cyclin E-YFP fusion protein is shown in red (graph, bottom panel). B: YFP (lane 1) or the cyclin E-YFP fusion protein (lane 2) were co-transfected with HA-tagged Cul3 and immunoprecipitated using HA antibody. IP results are shown in the top panel. The two lower panels show relative amounts of protein in each of the original samples. Migration of size markers indicated to the right of gel images (kDa).

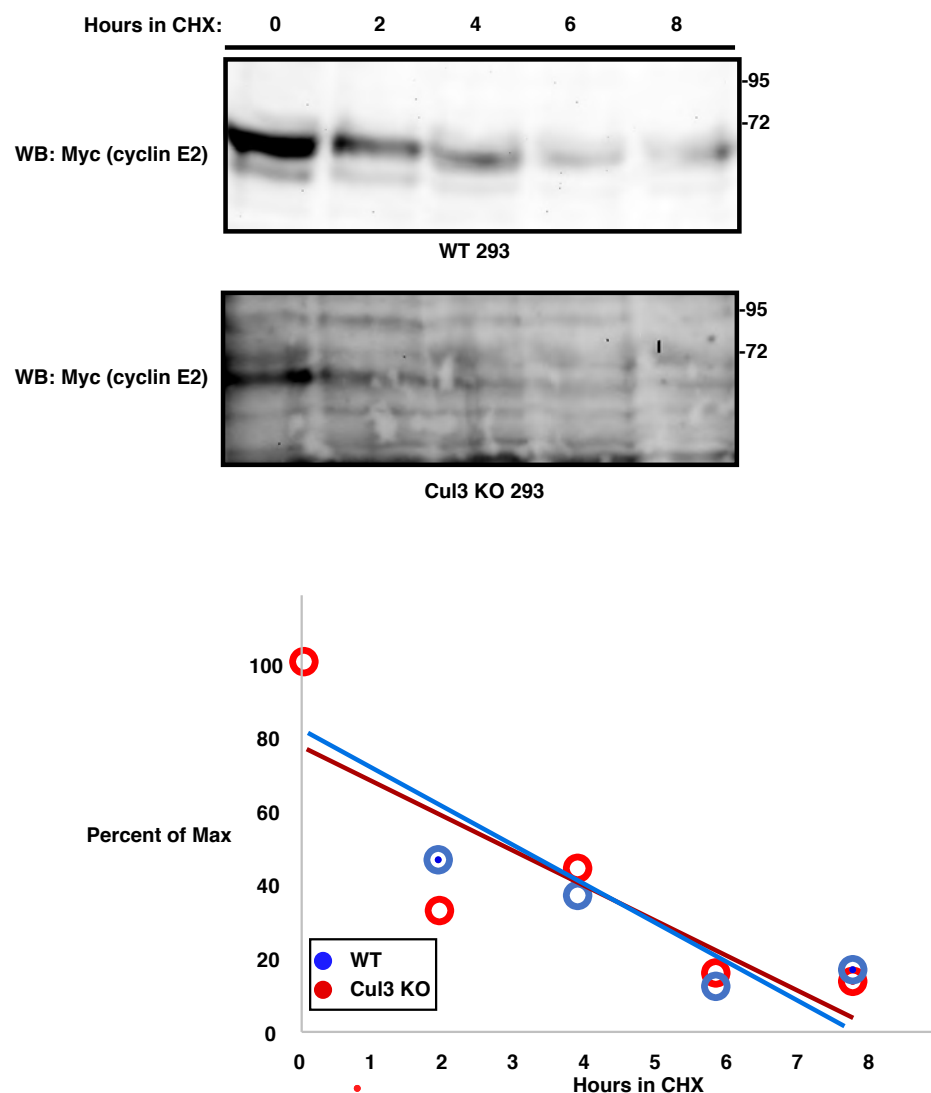


**Figure S5:** Cul3 has no effect on the half-life of cyclin E2. WT and Cul3KO 293 cells were transfected with Myc-cyclin E2. Cycloheximide was added 24 hours post-transfection and cells were harvested every two hours following cycloheximide addition. Top panel: Western blots showing protein expression levels. Migration of size markers indicated to the right of gel images (kDa). Lower panel: plot of half lives as percent of maximum signal.